

# *Geological Field Trips and Maps*

2018

Vol. 10 (2.2)



ISSN: 2038-4947

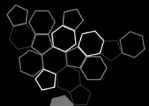


*Società Geologica  
Italiana*



**ISPRA**

Dipartimento per il  
**SERVIZIO GEOLOGICO D'ITALIA**  
Organo Cartografico dello Stato (legge n°68 del 2-2-1960)



Sistema Nazionale  
per la Protezione  
dell'Ambiente

**Field trip to the Ischia resurgent caldera,  
a journey across an active volcano in the Gulf of Naples**

Cities on Volcanoes 10 Meeting – Napoli 2018

<https://doi.org/10.3301/GFT.2018.03>

## GFT&M - *Geological Field Trips and Maps*

Periodico semestrale del Servizio Geologico d'Italia - ISPRA e della Società Geologica Italiana  
Geol. F. Trips Maps, Vol. **10** No.2.2 (2018), 000 pp., 00 Figs. (<https://doi.org/10.3301/GFT.2018.03>)

### Field trip to the Ischia resurgent caldera, a journey across an active volcano in the Gulf of Naples

#### Cities on Volcanoes 10 Meeting – Napoli 2018

**Fabio Sansivero<sup>1</sup>, Sandro de Vita<sup>1</sup>, Enrica Marotta<sup>1</sup>**

With contributions of:

**Fabio Sansivero<sup>1</sup>, Sandro de Vita<sup>1</sup>, Enrica Marotta<sup>1</sup>, M. Della Seta<sup>2</sup>, S. Martino<sup>2</sup>, G.M. Marmoni<sup>2</sup>**

<sup>1</sup> Istituto Nazionale di Geofisica e Vulcanologia, Sezione di Napoli Osservatorio Vesuviano

<sup>2</sup> Dipartimento di Scienze della Terra, Università di Roma La Sapienza

Corresponding Author e-mail address: [fabio.sansivero@ingv.it](mailto:fabio.sansivero@ingv.it)

Responsible Director

*Claudio Campobasso* (ISPRA-Roma)

Editor in Chief

*Andrea Zanchi* (Università di Milano-Bicocca)

Editorial Manager

*Mauro Roma* (ISPRA-Roma) - corresponding manager

*Silvana Falcetti* (ISPRA-Roma), *Fabio Massimo Petti* (Società Geologica Italiana - Roma),

*Maria Luisa Vatovec* (ISPRA-Roma), *Alessandro Zuccari* (Società Geologica Italiana - Roma)

Associate Editors

*M. Berti* (Università di Bologna), *M. Della Seta* (Sapienza Università di Roma),

*P. Gianolla* (Università di Ferrara), *G. Giordano* (Università Roma Tre), *M. Massironi*

(Università di Padova), *M.L. Pampaloni* (ISPRA-Roma), *M. Pantaloni* (ISPRA-Roma),

*M. Scambelluri* (Università di Genova), *S. Tavani* (Università di Napoli Federico II)

Editorial Advisory Board

*D. Bernoulli, F. Calamita, W. Cavazza,*

*F.L. Chiocci, R. Compagnoni,*

*D. Cosentino, S. Critelli, G.V. Dal Piaz,*

*P. Di Stefano, C. Doglioni, E. Erba,*

*R. Fantoni, M. Marino, M. Mellini,*

*S. Milli, E. Chiarini, V. Pascucci,*

*L. Passeri, A. Peccerillo, L. Pomar,*

*P. Ronchi, B.C. Schreiber, L. Simone,*

*I. Spalla, L.H. Tanner, C. Venturini,*

*G. Zuffa.*

ISSN: 2038-4947 [online]

<http://gftm.socgeol.it/>

The Geological Survey of Italy, the Società Geologica Italiana and the Editorial group are not responsible for the ideas, opinions and contents of the guides published; the Authors of each paper are responsible for the ideas, opinions and contents published.

Il Servizio Geologico d'Italia, la Società Geologica Italiana e il Gruppo editoriale non sono responsabili delle opinioni espresse e delle affermazioni pubblicate nella guida; l'Autore/i è/sono il/i solo/i responsabile/i.

INDEX

Information

Abstract ..... 4  
 Information ..... 4  
 Field trips summary ..... 5

Excursion notes

Geological setting ..... 8

Itinerary

**1st day – Circumnavigation of the island** ..... 19  
**Stop 1.1:** Northern sector of Mt. Epomeo and Casamicciola area ..... 19  
**Stop 1.2:** From Punta La Scrofa to Ischia Porto..... 19  
**Stop 1.3:** From Punta Molina to Carta Romana ..... 22  
**Stop 1.4:** From Grotta del Mago to Punta San Pancrazio .. 24  
**Stop 1.5:** From Punta San Pancrazio to Punta della Signora..... 25  
**Stop 1.6:** Maronti beach and Mt. Epomeo southern slope . 27  
**Stop 1.7:** Sant’Angelo and Sorgeto ..... 28  
**Stop 1.8:** From Capo Negro to Punta Imperatore ..... 31

**Stop 1.9:** The Forio area and the western slope of Mt. Epomeo ..... 32  
**Stop 1.10:** From Zaro promontory to Mt. Vico ..... 33

**2nd day – Recent volcanic activity at Ischia** ..... 35

**Stop 2.1:** The Rotaro volcanic complex..... 35  
**Stop 2.2:** The Montagnone-Maschiata volcanic complex and the deposits of recent volcanic activity ..... 38  
**Stop 2.3:** The Arso crater ..... 40  
**Stop 2.4:** The Rio Corbore lava flow ..... 41  
**Stop 2.5:** The Serrara belvedere..... 42  
**Stop 2.6:** The Zaro area ..... 44

**3rd day – The Mt. Epomeo: caldera-forming eruptions, volcano-tectonic evolution and slope-instability** ..... 46

**Stop 3.1:** Purgatorio locality: the Mt. Nuovo DSGSD..... 46  
**Stop 3.2:** The Forio area: Debris avalanches and lahars of the western slopes of Mt. Epomeo..... 49  
**Stop 3.3:** Pietra Martone and Bosco della Falanga ..... 52

References ..... 56

## Abstract

Ischia is one of the most impressive examples of post-caldera resurgence in the world, with its almost 1,000 m of uplift in less than 30 ka. This three-days field trip will lead the participants through the geological and volcanological history of the island, illustrating the volcanic and related hazardous phenomena threatening about 50,000 inhabitants. Effusive and explosive eruptions, catastrophic earthquakes and huge debris-avalanches struck the island that, since Neolithic times, experienced a complex history of alternating human colonization and natural disasters.

The field trip consists of three routes: 1) the circumnavigation of the island, aimed to outline its main volcanological, geomorphological and tectonic features and to observe the oldest volcanic rocks exposed, stimulating discussions about coastal evolution and the relationships between volcanism, volcano-tectonism and slope instability; 2) an onland excursion on peculiar aspects of the products related to Ischia more recent period of volcanic activity; 3) a route focusing on the Mt. Epomeo Green Tuff caldera forming eruptions (55-60 ka), encouraging a discussion on the dynamics of the intracalderic resurgence and the geomorphological evolution of the Mt. Epomeo slopes, with ongoing Mass Rock Creep (MRC) processes culminating in rock-avalanche, debris-avalanche and lahar deposits.

Key words: *Ischia volcano, volcanic products, volcano-tectonics, caldera resurgence, volcanism.*

## INFORMATION

### General information

### Emergency contact numbers, hospitals and first-aids

112 - Carabinieri

113 - Police

115 - Fire fighters

118 - First Aid

Hospital ANNA RIZZOLI, via Fundera - 80076 Lacco Ameno. Phone: 0815079111 - 0815079231

Ambulance Croce Bianca, 80076 Lacco Ameno. Phone: 081983022 - 360272541

## Field trips summary

### 1<sup>st</sup> day - Circumnavigation of the island

Significance: the view from the sea is the best way to have a quite comprehensive portrait of the deposits, landforms and structural evidence related to both ancient and recent evolution of Ischia island.

Discussion points: although the discussion points can be numerous, due to the wide area observed, the debate can be stressed on the difficulties encountered in studying and quantifying the characteristics of volcanic and epiclastic deposits of an island, as it is almost always impossible to follow them beyond the coast line.

### 2<sup>nd</sup> day - Recent volcanic activity at Ischia

#### *Stop 2.1 The Rotaro volcanic complex*

Significance: evolution of the Rotaro volcanic complex, one of the rare cases of post-caldera polygenic volcanoes at Ischia.

Discussion points: the Ischia polygenic volcanoes and their relationships with the main magma feeding-structures of the island.

#### *Stop 2.2 The Montagnone-Maschiata volcanic complex and the deposits of the most recent volcanic activity (last 10 ka)*

Significance: evolution of Montagnone-Maschiata volcanic complex and recent explosive activity in the north-eastern area of Ischia (Cretaio, Bosco dei Conti, Posta Lubrano and Cava Bianca Tephra).

Discussion points: Cretaio Tephra, the highest-magnitude eruption of the last 10 ka volcanic activity.

#### *Stop 2.3 The Arso crater*

Significance: the 1302 AD Arso eruption, the last volcanic activity at Ischia. Lava flow morphology and areal distribution.

Discussion points: a future eruption in the densely inhabited eastern sector of Ischia island: impact, risk and mitigation actions.

### *Stop 2.4 The Rio Corbore lava flow and Piano Liguori Tephra*

Significance: Rio Corbore lava front, structures and rheology of a high aspect ratio lava flow; the Piano Liguori Tephra outcrop at Spalatriello locality and volcanic landforms of the last 10 ka in the south-eastern sector of the island.

Discussion points: different areal distribution of major last 10 ka explosive eruption at Ischia. Hazard and impact implications.

### *Stop 2.5 The Serrara belvedere*

Significance: the morphological evolution of the Serrara-Fontana area and the remobilization of the sedimentary and epiclastic deposits mantling the southern slopes of the Mt. Epomeo resurgent block. The Chiarito Tephra, a greek-age eruption in the south-western sector of the island.

Discussion points: relationships between subaerial debris avalanche deposits, submarine landslide deposits and volcano-tectonics. Volcanic activity outside the eastern sector of the island, implications in the volcanic hazard assessment (part I).

### *Stop 2.6 The Zaro area*

Significance: the Zaro lava field, vent alignment and lava flow morphology, mineralogical and textural characteristics.

Discussion points: lava flow rheology and high aspect ratio lava bodies. Volcanic activity outside the eastern sector of the island, implications on the volcanic hazard assessment (part II).

## **3<sup>rd</sup> day - The Mt. Epomeo: caldera-forming eruptions, volcano-tectonic evolution and slope-instability**

### *Stop 3.1 Purgatorio locality: the Mt. Nuovo DSGSD (Deep Seated Gravitational Slope Deformation)*

Significance: the morphological diagnostic features, which identify the Mt. Nuovo DSGSD as an ongoing Mass Rock Creep (MRC) process, its structural model, and relationships with resurgence and geothermal system.

Discussion points: possible scenario for the Mt. Nuovo landslide evolution (slope failure and related tsunamis); relationships between renewal of magmatic activity, phreatic eruptions and catastrophic debris/rock avalanches.

### *Stop 3.2 The Forio plain: Debris avalanches and lahars from the western slopes of Mt. Epomeo*

Significance: the Falanga debris/rock avalanche and mass rock movements from western slopes of Mt. Epomeo resurgent block. The Forio Class 1 lahar. Local seismic response conditioned by volcanoclastic cover.

Discussion points: multi-hazard scenarios, relationships between seismicity, renewal of magmatic activity and catastrophic debris/rock avalanches from northern flanks of Mt. Epomeo.

### *Stop 3.3 Pietra Martone and Bosco della Falanga*

Significance: outcrops of intracaldera ignimbrite facies of the Mt. Epomeo Green Tuff.

Discussion points: large explosive eruptions at Ischia and Mt. Epomeo Green Tuff dispersion outside the island. Green Tuff caldera limits and shape.



## Geological setting

The island of Ischia, located at the north-western border of the Gulf of Naples, hosts an active volcanic field, which is included in the framework of the Tyrrhenian volcanism. This volcanism is connected to the Plio-Quaternary evolution of the western Mediterranean area, which is characterized by the anticlockwise rotation of the Italian peninsula, occurred during the interaction between the African and the European plates (Ippolito et al., 1973; D'Argenio et al., 1973; Finetti and Morelli, 1974; Bartole, 1984; Piochi et al., 2005). The activation of NW-SE normal faults and NE-SW normal to strike-slip transfer faults during this process, allowed the magmas to reach the surface, feeding the volcanism that is still active also in the other Neapolitan volcanoes (Somma-Vesuvius and Campi Flegrei caldera).

Ischia is only the emerging part of a much wider complex that rises about 1,000 m above the sea bottom (Fig. 1; Orsi et al., 1999; Bruno et al., 2002). It covers an area of 46.4 km<sup>2</sup> and reaches the maximum elevation of 787 m a.s.l. at Mt. Epomeo, which is located in the central part of the island. A minor alignment



Fig. 1 - 3D view of Ischia island with bathymetry (modified after Della Seta et al., 2012).



of peaks characterizes the south-eastern part of the island. The coast morphology alternates steep cliffs and promontories with sandy beaches and slopes that gently dip to the sea.

The rocks exposed on the island are mainly volcanic or landslide deposits and subordinate terrigenous sedimentary rocks that testify the alternation of constructive and destructive phases of morphogenesis, due to the interplay among volcanism, volcano-tectonism and diffuse episodes of slope instability (de Vita et al., 2006; 2010; Della Seta et al., 2012).

## Volcanological evolution

The beginning of volcanic activity at Ischia is not well defined, as the oldest dated rocks are not the lowermost exposed on the island. They have an age of about 150 ka and volcanism continued until the last eruption, occurred in 1302 AD, with intercalated centuries to millennia of quiescence (Vezzoli, 1988). The oldest exposed rocks (Scarrupata di Barano Formation; Vezzoli, 1988; Ancient Ischia Synthem; Sbrana and Toccaceli, 2011; Fig. 2) range in age between 150 and 74 ka and are lavas and pyroclastic deposits, representing the remnant of a partially eroded volcanic complex, exposed in the south-eastern part of the island, and small lava domes, exposed along the coasts. Between 74 and 55 ka a very intense period of explosive volcanism followed, likely producing the highest magnitude eruptions occurred on the island from vents mainly located along the southern coasts of Ischia (Brown et al., 2008; Rifugio di San Nicola Synthem; Sbrana and Toccaceli, 2011). This long lasting period of activity culminated between 60 and 55 ka with the caldera-forming eruptions that generated at least two or three ignimbritic deposits, known in the literature as the Mt. Epomeo Green Tuff (Brown et al., 2008 and references therein; Pizzone, Frassitelli and Mt. Epomeo Green Tuff of Sbrana and Toccaceli, 2011). The caldera collapse caused the submersion of the central part of the island, and these tuffs mainly constitute the caldera filling deposits, which were emplaced partially in a submarine environment and partially on land, outside the caldera margins. Since its formation the caldera depression became a basin of sedimentation, in which a sequence of volcanoclastic and terrigenous deposits formed by the reworking of the tuffs and sedimentary supply from the mainland (Sbrana and Toccaceli, 2011). After these caldera-forming eruptions, volcanism continued up to 33 ka with the activation of vents in the south-western and north-western offshore of the island, from which originated a series of high-energy hydromagmatic eruptions, whose deposits are presently exposed to the west of Mt. Epomeo. The intrusion of the magmas that fed these eruptions, very likely started the uplift of the caldera floor, causing the emersion of the Mt. Epomeo resurgent block.

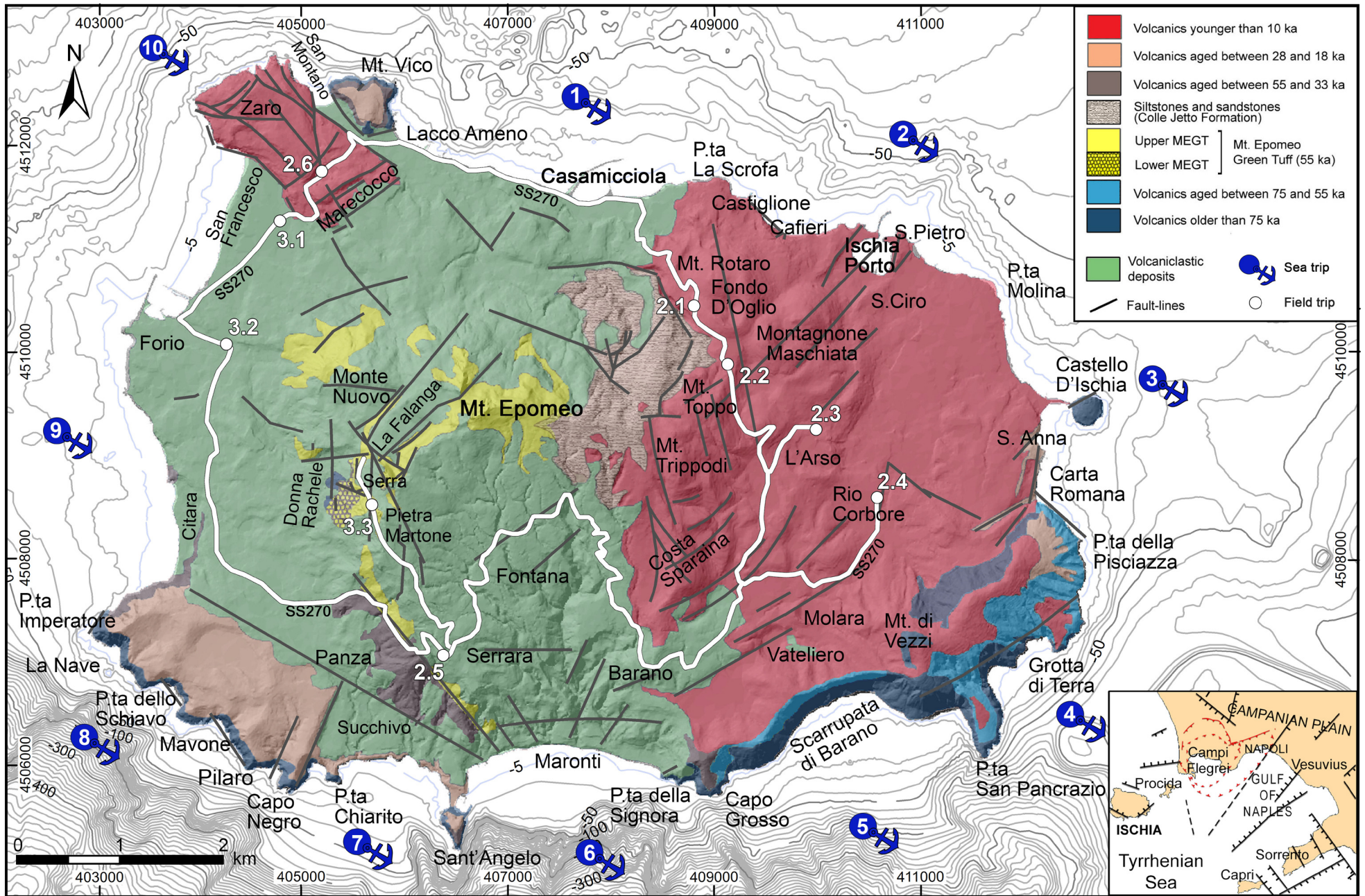


Fig. 2 - Geologic sketch map of Ischia with sea and field trips (modified after de Vita et al., 2010).



After a repose interval that lasted about 5 ka, volcanism resumed at 28 ka with a series of effusive and both phreatomagmatic and magmatic, low-energy explosive eruptions, which occurred sporadically until 18 ka. These eruptions produced lava flows, Strombolian fallout deposits and the building of small tuff-cones and scoria cones, currently exposed along the south-eastern and south-western coasts of the island (Campotese Subsynthem; Sbrana and Toccaceli, 2011).

The following time interval is of controversial interpretation in the literature, based on different radiometric datings of the outcropping volcanics. Vezzoli (1988) defines this period as a repose interval that lasted between 18 and 10 ka. More recent studies suggest that some eruptions occurred during this time span (Sbrana and Toccaceli, 2011). However, despite this discrepancy, almost all the authors agree in considering this time interval as a period of very reduced volcanic activity. On the contrary, the following period, started at 10 ka, was characterized by a very intense volcanic activity, mainly concentrated at around 5.5 ka and in the last 2.9 ka (de Vita et al., 2010). Almost all the eruption vents of this period are localized in the eastern part of the island. Only a few of these were activated outside this area, along regional faults or at the margins of the resurgent block. The last 2.9 ka of activity were characterized by at least 34 effusive and explosive eruptions. Effusive eruptions generated lava domes and usually high-aspect ratio lava-flows. Only the last eruption, occurred in 1302 AD produced a lava flow which had the mobility to travel as far as about 3 km. Explosive eruptions produced variably dispersed pyroclastic-fall and -current deposits with variable impact on human settlements and the environment, and built small tuff-cones and tuff-rings (de Vita et al., 2010 and references therein; Sbrana and Toccaceli, 2011; de Vita et al., 2013).

In the past 10 ka volcanism was characterized by the alternation of periods of very intense activity and long lasting intervals of quiescence (Fig. 3). Therefore, it has been hypothesized that episodes of magma intrusion and resurgence occurred intermittently (Tibaldi and Vezzoli, 2004; de Vita et al., 2006; Vezzoli et al., 2009; de Vita et al., 2010). In particular, during the past 5.5 ka the deposits related to surface gravitational movements preceded and followed the emplacement of the eruptions products, testifying that vertical movements related to resurgence that caused slope instability, occurred through the activation of the same faults that fed volcanism. According to de Vita et al. (2006) the emplacement of both large debris avalanche and minor landslide deposits occurred in four main phases of gravitational instability and volcanic activity, dated between 5.5 and 2.9 ka, around 2.9 ka, between 2.6 and 2.3 ka, and between 2.3 and 1.9 ka, respectively. Also the last eruption, occurred on the island in 1302 AD, was preceded by the activation of large mass movements, leading Della Seta et al. (2012) to hypothesize the occurrence of a possible fifth phase of slope instability.

Since the last eruption, no evidence of renewal of uplift have been recorded. Del Gaudio et al. (2010) based on radar interferometric data and levelling surveys, suggest that in very recent times only a low rate of subsidence is recordable at Ischia, likely due to the depressurization of the hydrothermal system and crack-closure processes (Manzo et al., 2006; Sepe et al., 2007). However, the historical time intense volcanism (de Vita et al., 2010), the presence of widespread fumaroles and thermal springs (Di Napoli et al., 2011) and seismic activity (Cubellis and Luongo, 1998) testify that at the present the Ischia magmatic system has to be considered still active.

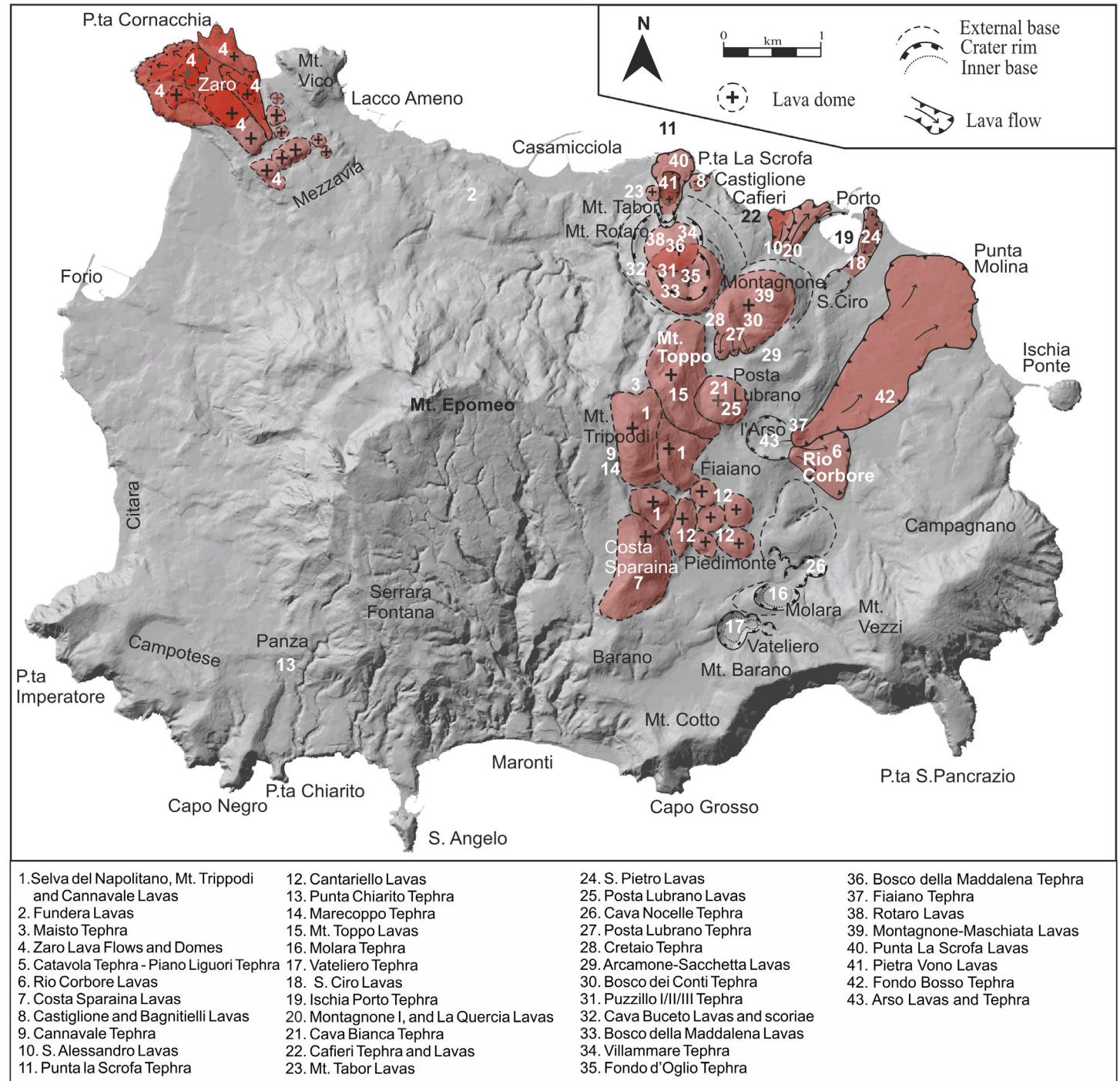


Fig. 3 – Location map of the active vents and areas covered by lavas ascribed to volcanic activity of the past 10 k (modified after de Vita et al., 2010).



## Resurgence

Ischia is one of the most impressive case of intracaldera resurgence in the world, with an about 1,000 m of uplift of its central part. The resurgent area is composed of a series of differentially displaced blocks, and is characterized by a polygonal shape, defined by the intersection of newly formed, volcano-tectonic faults, and regional faults reactivated during resurgence (Orsi et al., 1991; Acocella and Funiciello, 1999). The uplifted blocks are variably raised and inclined, with a general tilting of the entire area around a NE-SW oriented horizontal axis, located in the southeastern part of the resurgent area. The result is an asymmetric block structure, in which the most uplifted part is located in the northwestern sector of the resurgent area (Fig. 2; Rittmann and Gottini, 1980; Vezzoli, 1988; Orsi et al., 1991; Acocella and Funiciello, 1999; de Vita et al., 2006; de Vita et al., 2010; Della Seta et al., 2012). The western part of the resurgent area is bordered by N-S and NE-SW trending structures. To the east N-S, NE-SW and NW-SE trending faults define a series of blocks differentially lowered toward east. Toward north-northeast the limit of the resurgent area is not well defined, as still along the shoreline there are beach deposits displaced at different elevations above sea-level by E-W and NW-SE trending faults.

The beginning of resurgence, as well, is not precisely defined, although it is commonly accepted that it was related to the intrusion of new magma into the system (Rittmann, 1930; Rittmann and Gottini, 1980; Orsi and Chiesa, 1988; Orsi et al., 1991; Luongo et al., 1995; Tibaldi and Vezzoli, 1997; Tibaldi and Vezzoli, 1998; Acocella and Funiciello, 1999; Moli et al., 2003; Carlino et al., 2006; 2012), very likely occurred before the eruptions dated at 33 ka.

As already stated, geodetic data show a generalized subsidence of the uplifted block. This suggests that currently the resurgent phenomenon is at rest (de Vita et al., 2006; Manzo et al., 2006; Sepe et al., 2007; De Novellis et al., 2018).

## Magmatic system

The exposed volcanic rocks of Ischia belong to the low-K series of the Roman Comagmatic Province and range in composition from shoshonite to phonolite. The most abundant rocks are alkali-trachyte (Fig. 4a; Angiulli et al., 1985; Poli et al., 1987; Poli et al., 1989; Crisci et al., 1989; Civetta et al., 1991; Sbrana and Toccaceli, 2011; D'Antonio et al., 2013; Moretti et al., 2013; Casalini et al., 2017). According to Sbrana and Toccaceli (2011) the oldest outcropping rocks (150-75 ka) are trachytic in composition, with an alkali content and a Na<sub>2</sub>O/K<sub>2</sub>O ratio



that decrease over time. The highest magnitude explosive eruptions of this period had a phonolitic composition with higher  $\text{Na}_2\text{O}/\text{K}_2\text{O}$  ratio and higher peralkalinity index.

The period of activity included between 75 and 50 ka has been deepened inside by Brown et al. (2014). These authors evidenced that significant changes occurred in the magmatic system before and after the caldera-forming eruptions, and that it was periodically refilled by magmas of deep origin, characterized by different isotopic compositions. Before the Mt. Epomeo Green Tuff eruption, magmas were trachytic and phonolitic in composition, poorly enriched in radiogenic Sr and progressively less radiogenic with time. The eruptions that immediately preceded the Green Tuff were fed by an isotopically distinct magma and, as the Green Tuff itself, had a phonolitic-to-trachytic composition. Brown et al. (2004) estimate that an amount of about 5-10 km<sup>3</sup> of magma accumulated at a depth of 4-6 km in a 20 ka long time-span. Following the Green Tuff eruptions, volcanism was fed by a new and less differentiated magma, whose geochemical and Sr and Nd isotope variations bear witness to the ascent of distinct magma bodies, variably contaminated by a crystalline metamorphic basement. These magmas directly reached the surface or stagnate and differentiate at shallower depths, erupting during explosive eruptions (Brown et al., 2014).

During the past 50 ka the magmatic system behaved in a complex way, being characterized by phases of evolution in closed-system conditions that alternate with phases in which new and isotopically distinct magmas entered the system, recording evidence of contamination and mixing processes with resident magmas. Magma composition and eruptive dynamics of the post-Green Tuff activity, are significantly different from the previous periods. The erupted magmas were shoshonitic and latitic in composition (Civetta et al., 1991; Brown et al., 2008; 2014), and the eruptions show a progressively increasing water/magma interaction that culminated with the eruptions of the Citara Formation (Rittmann, 1930; Rittmann and Gottini, 1980; Vezzoli, 1988; Tufi di Citara in Sbrana and Toccaceli, 2011).

The magmas that fed the eruptions included between 28 and 18 ka vary in composition with time from shoshonite to alkali-trachyte, with increasing incompatible elements content and Sr isotopic ratio. This variability has been interpreted as the evidence of the arrival of a new basic magma into the volcanic system and its progressive differentiation and mixing with the resident magma (Civetta et al., 1991).

Civetta et al. (1991) evidenced that the last period of volcanic activity at Ischia (10 ka BP - 1302 AD) was characterized by a well evident decrease in the value of Sr isotopic composition, and interpreted it as reflecting the arrival of a geochemically distinct magma into the system. The erupted products are mostly trachytic and subordinately latitic, with a negative correlation between chemical and isotopic composition. Piochi et al. (1999) stated that chemical and isotopic variations of all the rocks of this period, and mineralogical disequilibria



of the less evolved products are evidence of mixing among different magmas either in the deepest part of the magmatic system or during the ascent of melts. At the present, according to the available geological and petrological data (Civetta et al., 1991; Orsi et al., 1996; Piochi et al., 1999), the magmatic system of Ischia seems to be composed of a deep and poorly-evolved magma reservoir, interconnected with shallower, smaller and more-evolved magma batches (also evidenced by the modelling of magnetic data; Orsi et al., 1999).

Starting from the geochemical and isotopic analysis of a set of samples representative of almost all the outcropping Ischia products, Casalini et al. (2017), showed that long period of permanence in magma chambers are required to justify the anomalous Sr isotopic ratios of some products. They also demonstrated, reconstructing the isochrones on the basis of Rb and Sr contents, that the time of residence of magmas before eruptions, range from a few tens to hundreds and thousands of years (Fig. 4b).

The studies conducted on the more mafic products of the pas 10 ka by D'Antonio et al. (2013) and Moretti et al., (2013) converge to the hypothesis of generation of magmas mainly dominated by gas-fluxing of CO<sub>2</sub> in a mantle modified by crustal assimilation. This process should be demonstrated by typically mantellic dO<sup>18</sup> values and a Sr isotopic ratio that increases towards crustal values.

## Slope instability

Volcanism and volcano-tectonism at Ischia were strictly linked with slope instability at least in the past 10 ka. Deposits related to the gravitational instability of both coastal and resurgent block slopes involved very variable volumes of rocks and debris, remobilized by different landslide mechanisms.

These characteristics allowed to classify slope instability phenomena in two categories: i) large rock and debris landslides and ii) impulsive shallow landslides.

The first category includes rock avalanches, due to the collapse of entire portions of slopes that deform over a long-time scale (10<sup>4</sup>-10<sup>5</sup> years; Mass Rock Creep; Chigira, 1992), or debris avalanches related to impulsive triggers. The second one includes smaller landslides, such as rock failure, roto/translational slides and earth/debris flows and lahars (volcanoclastic debris flows), triggered by volcanic eruptions, phreatic explosions and earthquakes, or by meteo-climatic events (Catenacci, 1992; Del Prete and Mele, 1999; 2006; Tibaldi and Vezzoli, 2004; de Vita et al., 2006; Della Seta et al., 2012 and references therein; Di Martire et al., 2012).

In Fig. 5 are reported the chronostratigraphic relationships between large rock and debris avalanches, impulsive shallow landslides and volcanic deposits (Della Seta et al., 2012).

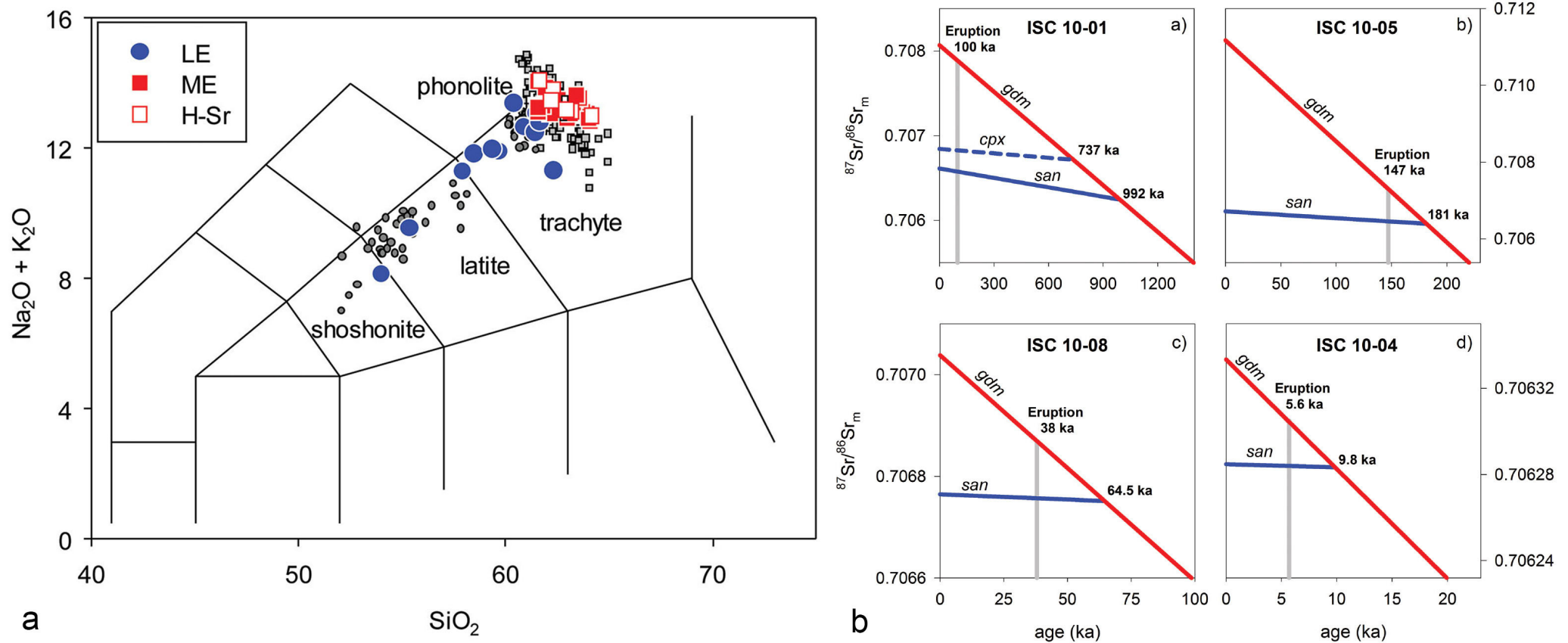


Fig. 4 – a) TAS diagram of the Ischia volcanics. Solid circles are referred to less-evolved samples (LE), solid squares to more-evolved samples (ME) and open squares represent a sub-group of more evolved samples (H-Sr) with anomalous radiogenic  $^{87}\text{Sr}/^{86}\text{Sr}$  (modified after Casalini et al., 2017). Gray circles and squares are literature data. b) isochrones reconstruction in  $^{87}\text{Sr}/^{86}\text{Sr}_m$  vs. age plots of selected samples with both anomalous (a and b), and normal (c and d) whole-rock  $^{87}\text{Sr}/^{86}\text{Sr}$  (modified after Casalini et al., 2017). Straight lines represent groundmass (gdm) and minerals (san = sanidine, cpx = clinopyroxene) backward evolution of  $^{87}\text{Sr}/^{86}\text{Sr}$  based upon their respective  $^{87}\text{Rb}/^{86}\text{Sr}$ . The intersection yields the mineral crystallization age and the mineral residence time is calculated by subtracting the K-Ar eruption age.

Landslide deposits intercalated with volcanic deposits younger than 10 ka (Tibaldi and Vezzoli, 2004; de Vita et al., 2006) are concentrated in the eastern and southern sectors of the island. The northern and western sectors are characterized by the outcrop of huge landslide deposits, likely emplaced as rock avalanches generated by MRC (Fig. 6), that are mainly part of the historical record (Della Seta et al., 2012; and references therein). The most intense

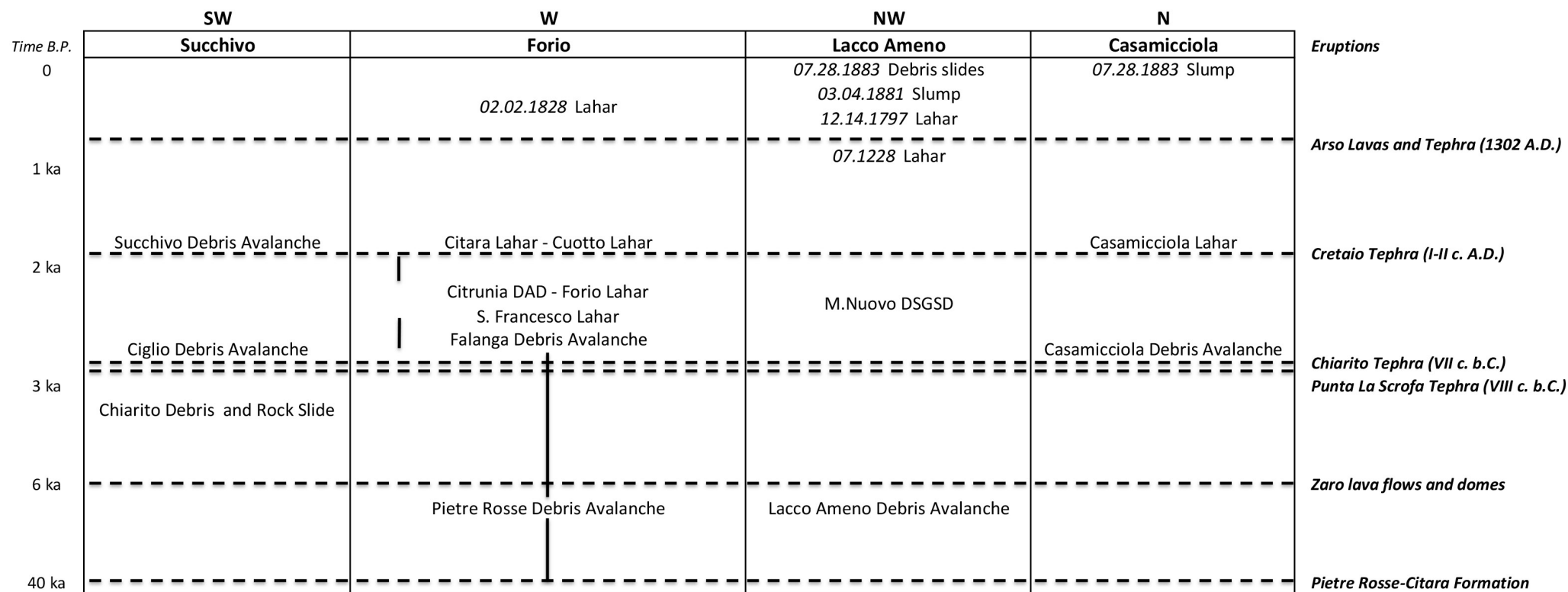


Fig. 5 - Time distribution of the slope gravitational events for Ischia, in relation to primary volcanic deposits (dotted lines) and grouped according to the impact area (modified after Della Seta et al., 2012).

phenomenon recorded on the island is a rock avalanche detached from the western side of Mount Epomeo (Della Seta et al., 2012; Sbrana and Toccaceli, 2011), with a volume estimated at 125 million m<sup>3</sup>. A deep seated gravitational slope deformation (DSGSD), likely related to MRC process is also reported as affecting the Monte Nuovo, on the western slope of Monte Epomeo (Fig. 6) in historical reports (Del Prete and Mele, 2006; and references therein). Geological and historical evidence of impulsive shallow landslides are reported by Di Martire et al. (2012), which collected the historical record, consisting in 288 individual landslide events, of which 23 occurred between the fourth century B.C. and 1924 and 255 between 1970 and 2010, with a temporal registration gap between 1924 and 1970 (Del Prete and Mele, 2006). The most recurrent typologies are represented by rock falls/topples, slides, flows and complex landslides (Fig. 7). Most of them are represented by flows (debris- or mud flow), which are concentrated within gullies, and by rock falls/topples, which affect the steepest slopes of Mount Epomeo

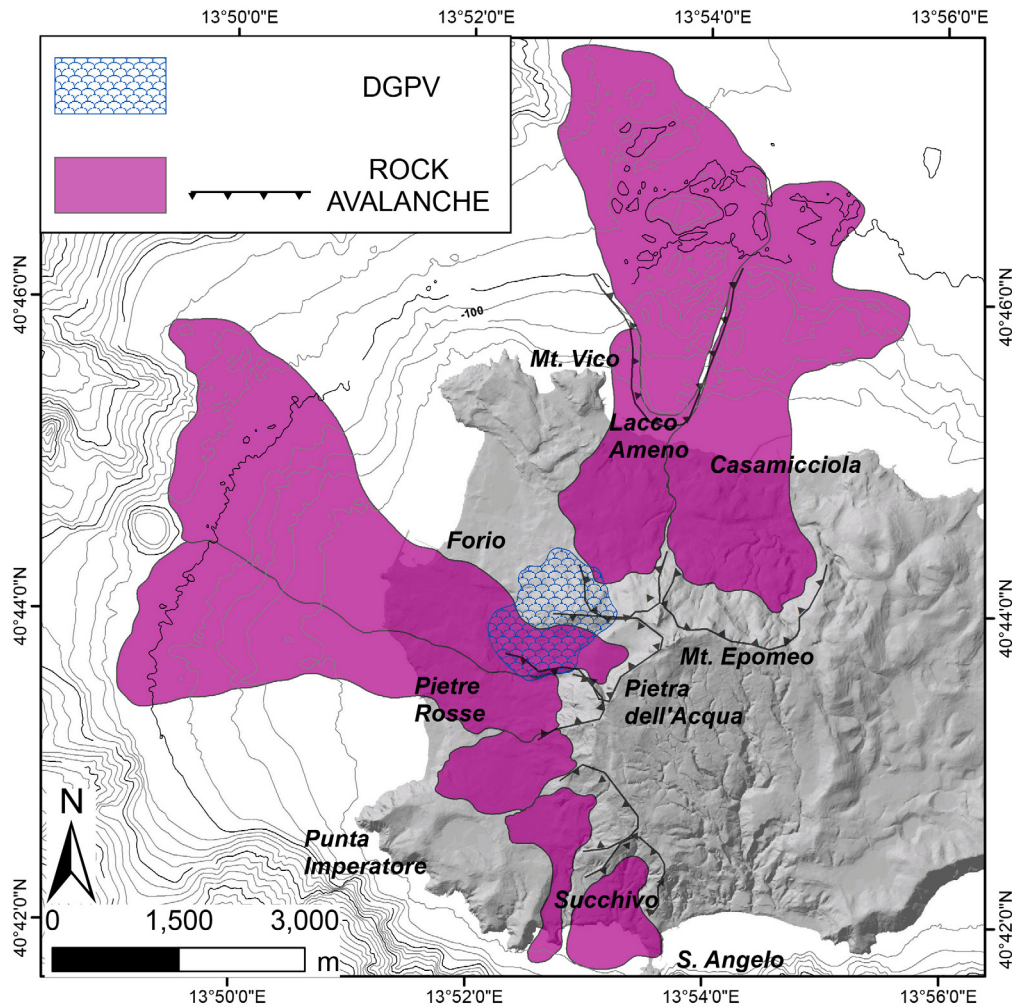


Fig. 6 - Spatial distribution of the rock avalanche deposits and of the ongoing MRC in the western sector of Mount Epomeo (modified after Della Seta et al., 2012).

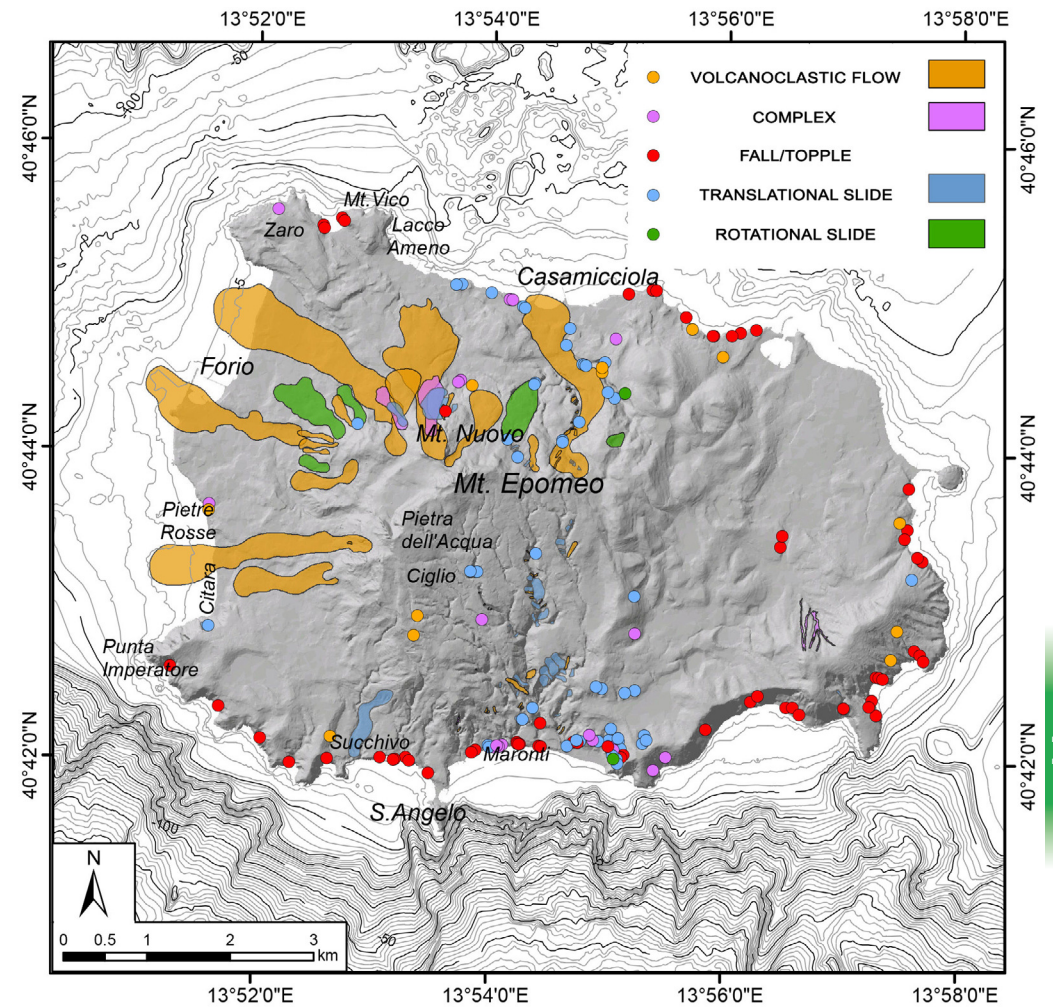


Fig. 7 - Spatial distribution of the impulsive landslides, including the debris avalanche IDA, at Ischia (modified after Di Martire et al., 2012).

and, above all, the sea cliffs (Catenacci 1992, Del Prete and Mele, 1999). Some events were chronologically constrained by stratigraphic relations with other landslide deposits and/or pyroclastic deposits (de Vita et al., 2006), while others were associated with the earthquakes of 1228, 1797, 1828, 1881, 1883 (Della Seta et al., 2012; and references therein).



## 1<sup>st</sup> day - Circumnavigation of the island

F. Sansivero<sup>1</sup>, S. de Vita<sup>1</sup>, E. Marotta<sup>1</sup>, M. Della Seta<sup>2</sup>, S. Martino<sup>2</sup>, G.M. Marmoni<sup>2</sup>

<sup>1</sup> Istituto Nazionale di Geofisica e Vulcanologia, Sezione di Napoli Osservatorio Vesuviano

<sup>2</sup> Dipartimento di Scienze della Terra, Università di Roma La Sapienza

Sailing around the Ischia island is undoubtedly the best way to view the deposits related to the ancient volcanic activity (150-18 ka), exposed along marine cliffs. It also gives the opportunity to identify some volcanic edifices and slope-instability deposits, produced during the last period of activity (10 ka - 1302 AD).

### Stop 1.1: Northern sector of Mt. Epomeo and Casamicciola area

The coast between Lacco Ameno and Casamicciola is mainly characterized by deposits correlated to at least two large episodes of rock-avalanche from the northern slope of Mt. Epomeo (Della Seta et al., 2012; Sbrana and Toccaceli, 2011). The famous mushroom-shaped rock of Lacco Ameno, is a Green Tuff hummock, modelled by sea erosion, that was carried and deposited by a rock-avalanche older than 6 ka (Fig. 8). Several historical debris-flow and mud-flow deposits, triggered by earthquakes and heavy rain episodes, overlie the rock-avalanche deposits. Historical chronicles reported more than 15 episodes of rock fall, debris slide and flash flood in the area of Casamicciola, with loss of life in the last ten decades (Santo et al., 2012). The last flood episode occurred in 2009 and caused one victim and twenty injured.

Casamicciola is the area of Ischia mostly affected by historical seismicity. More than 13 major earthquakes occurred in this area since 1228, with two catastrophic events in 1881 and 1883 (Cubellis and Luongo, 1998). These events were followed by a period of low seismic activity, which culminated on August 21, 2017 with a new earthquake of  $M_d = 4.0$  (De Novellis et al., 2018; Nappi et al., 2018). The seismicity is typically characterized by shallow hypocentres, moderate energy and high macroseismic intensity in a very limited area.

### Stop 1.2: From Punta La Scrofa to Ischia Porto

East of Casamicciola Harbour the coast is made of deposits related to the more recent period of volcanic activity (last 10 ka), which are overlain by mud-flow and debris-flow deposits. At Punta La Scrofa promontory, layered pyroclastic currents and subordinate fallout deposits are clearly visible (Punta La Scrofa Tephra; de Vita et al.,



Fig. 8 - Mushroom-shaped Green Tuff rock of Lacco Ameno (a); view of the northern slope of Mt. Epomeo from the sea at Lacco Ameno (b).

2010). They are dated 8th century BC as pottery fragments of this age were found at the base and inside the deposits. The geometry of the layers, bomb sags and sedimentological evidence suggest they are part of a tuff-cone likely located in the offshore, a few hundreds of meters north of Punta La Scrofa.

These deposits are overlain by two lava-flow units which are the last products of the Rotaro composite volcano, one of the two examples of polygenetic volcanic edifice of the last 10 ka at Ischia.

To the east of Punta la Scrofa, at Castiglione locality, highly fractured and foliated dark-grey lavas are exposed along the coast. These lavas are part of a lava-dome, which is coeval with a dyke, exposed at sea level at Bagnitielli locality. On the top of the lava dome a Bronze Age village (14th century BC) was found, partially buried by the previous mentioned pyroclastic deposits.

The coast between Bagnitielli and Ischia Porto shows a complex sequence (Fig. 9; de Vita et al, 2010) of volcanic and sedimentary deposits. To the west, the Castiglione Lavas and Bagnitielli Dyke (A, Fig. 9) are the oldest exposed deposits. Towards east the base of the sequence is composed of fossiliferous siltstones (SF, Fig. 9) overlain by a beach deposit (Sp, Fig. 9) that contains pottery dated at the 8th century BC. In the middle part



of the sequence, the products of the local eruptive vent of Cafieri are exposed. They are composed of fine-ash and pumice-lapilli pyroclastic-current layers ( $C_1$ , Fig. 9), and a thin lava-flow and scoriae bed ( $C_2$ , Fig. 9), which represent the latest episodes of activity of this vent, whose neck ( $N$ , Fig. 9) is still partially visible. Pyroclastic fallout deposit with subordinate pyroclastic-currents beds, related to Posta Lubrano Tephra ( $D$ , Fig. 9), Bosco della Maddalena Tephra ( $F$ , Fig. 9) and Cretaio Pyroclastics ( $E$ , Fig. 9) are exposed at the top of the sequence. The first two deposits originated from the Posta Lubrano and Rotaro volcanic vents, respectively. The Cretaio Pyroclastics (dated between the 1<sup>st</sup> century b.C and the 1<sup>st</sup> century A.D.) is the product of the highest magnitude eruption in the past 10 ka. Toward the east the Cafieri pyroclastic-current beds overly a paleosol dated 6<sup>th</sup>-5<sup>th</sup> century BC ( $P$ , Fig. 9), which develops above the S. Alessandro Lavas. These lavas are the lowermost unit of the volcanic succession exposed up to Ischia Porto. The top of this sequence is composed of a pyroclastic deposit, the Bosco dei Conti Tephra ( $G$ , Fig. 9), originated by the Montagnone volcanic complex (de Vita et al., 2010). The harbour of Ischia is a volcanic crater (Fig. 10b, c), formed during an explosive eruption occurred in the 5<sup>th</sup> century BC (the Ischia Porto eruption; de Vita et al., 2013). Originally it was a crater lake, separated from the sea by an isthmus of land, which was removed in 1854 by order of the king of the Two Sicilies Ferdinand II, to create the currently active harbour structure. The eruption was very low energetic and fed by a small volume

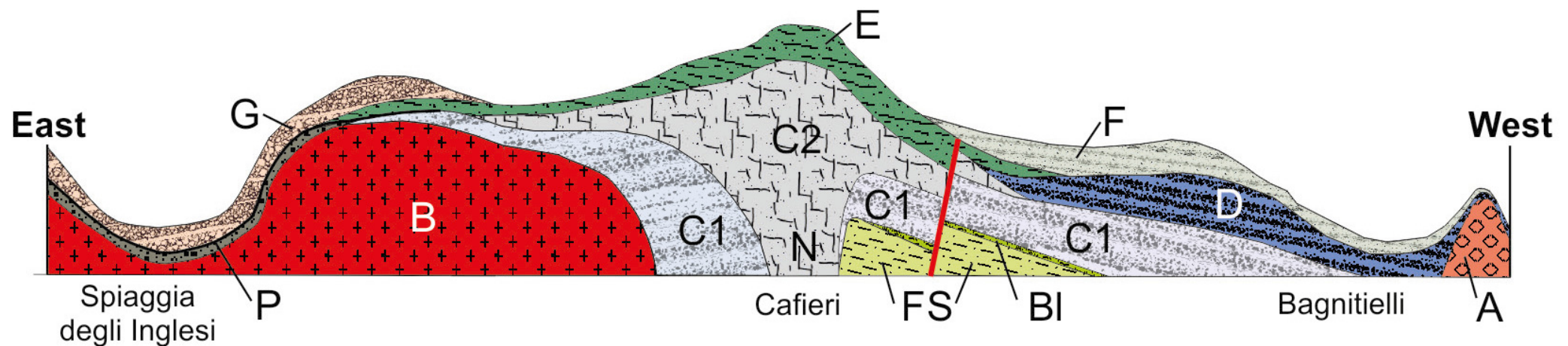


Fig. 9 - Sketch of the coast between Bagnitielli and Spiaggia degli Inglesi (modified after de Vita et al., 2010). A = Castiglione Lavas and Bagnitielli Dyke, B = San Alessandro Lavas, C1-C2 = Cafieri eruptive centre, D = Posta Lubrano Tephra, E = Cretaio Pyroclastics, F = Bosco della Maddalena Tephra, G = Bosco dei Conti Tephra, P = Paleosol dated 6<sup>th</sup>-5<sup>th</sup> century b.C., FS = Fossiliferous Siltstones, BI = Beach deposit dated 8<sup>th</sup> century b.C.



of magma. It was characterized by the alternation of phreatomagmatic and magmatic phases, which produced dilute and turbulent pyroclastic density currents, and Strombolian scoria fallout deposits (Fig. 10a), dispersed in a radius of a few hundred meters around the crater.

To the west of the harbour entrance, welded scoria layers (SCP, Fig. 10b), belonging to the Ischia Porto eruption, overlie the La Quercia lava flow (LQ; Fig. 10b), erupted during the early stages of formation of the Montagnone volcanic complex. To the east of the harbour entrance the small hill of S. Pietro is made of two superimposed lava flows, older than the Ischia Porto eruption: the S. Ciro Lavas (SC, Fig. 10b) at the base and the S. Pietro Lavas (SP, Fig. 10b) at the top. The first lava flow was emitted by a vent morphologically recognizable to the South of the harbour, the second one was likely a viscous lava body extruded locally. At the top of the S. Pietro hill, the remnants of building materials, related to the construction of a temple, were found. As reported by the Strabo's historical chronicles, the construction was abandoned between 474 and 466 BC by the Greek garrison of Syracuse due to the violent earthquakes that preceded the Ischia Porto eruption (Buchner, 1986; de Vita et al., 2013).

The volcanic edifice at SW of Ischia Porto, well visible when approaching the harbour by sea, is the Montagnone-Maschiata volcanic complex.

### Stop 1.3: From Punta Molina to Carta Romana

Sailing toward East, at Punta Molina the flow-front of the Arso Lavas is exposed along the shoreline. These lavas are the product of the last eruption occurred on the island in 1302 A.D. (Fig. 11).

Rounded Punta Molina the view is caught by the Castello d'Ischia lava dome, place of a suggestive Aragonese castle (Fig. 12). This lava dome is one of the older volcanic products of the island (dated  $\sim 130$  ka). The interpretation of this edifice is controversial, as some authors classified it as a welded-scoriae cone (Rittmann and Gottini, 1980; Sbrana and Toccaceli, 2011). A NE-SW trending fault exposes the inner structure of the edifice, characterized by flow foliation or strata of welded scoriae, depending on the given interpretation. The lava body is overlain by several pyroclastic deposits, belonging to explosive activity occurred between 73 and 59 ka (Sbrana and Toccaceli, 2011). At least three paleosols are well visible.

The coast of S. Anna, to the west and south-west of Castello d'Ischia, is composed of a sequence of scoriaceous lava flows (S. Anna Lavas, 23 ka) likely erupted on land. At Carta Romana these lavas cover a sequence of pyroclastic-fallout and -current deposits (Carta Romana Pyroclastics), alternated with several paleosols, belonging to the

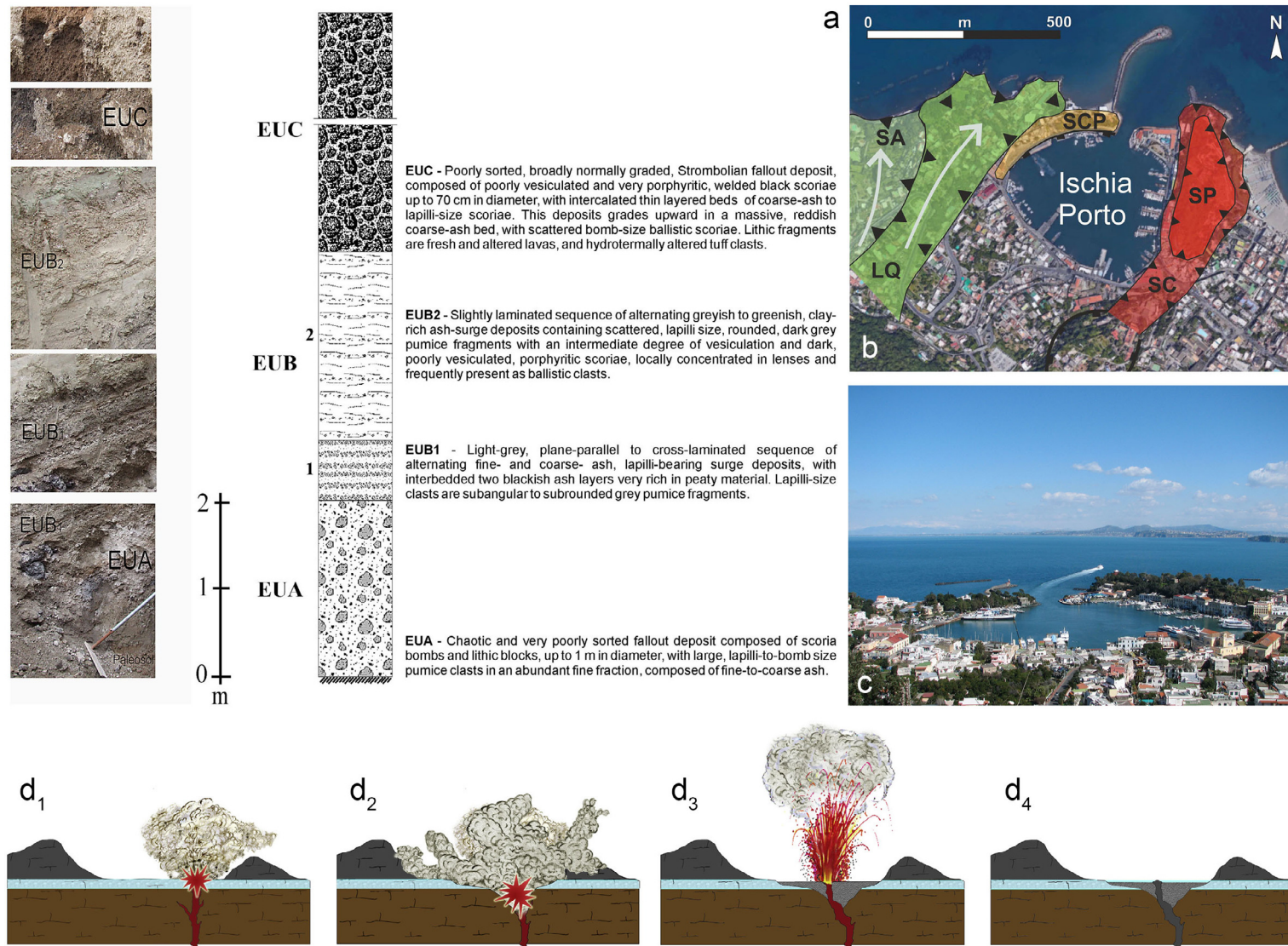


Fig. 10 - Ischia Porto eruption (5th century BC; modified after de Vita et al., 2013). a) Description and pictures of type section; b) area morphology sketch map: SA = S. Alessandro Lavas, LQ = La Quercia Lavas, SCP = Ischia Porto welded Scoriae, SC = S. Ciro Lavas, SP = S. Pietro Lavas; c) view of the harbour from Montagnone hill. Eruption history: d1) opening phase; d2) main phreatomagmatic phase; d3) Strombolian phase; d4) emplacement of the lava plug within the crater.



Fig. 11 - Limits and flow directions (a) of the lava flow emitted during the L'Arso eruption (1302 A.D). Arso Lavas outcrops at Punta Molina (b) with Procida island and Campi Flegrei in the background.

Ancient Ischia Synthem (~ 100 ka; Sbrana and Toccaceli, 2011). The S. Anna Lavas are overlain by the Piano Liguori Pyroclastics (5.5 ka; Orsi et al., 1996), which are a sequence of fine ash and pumice lapilli pyroclastic surges, produced by a phreatomagmatic eruption in Neolithic times. In all the Carta Romana area numerous submarine thermal springs are present. These springs were well known also to Romans which founded in this area the settlement of Aenaria, with villas, thermal pools and industrial activities. Nowadays the rests of this settlement are located at 5-7 metres below the sea level.

### Stop 1.4: From Grotta del Mago to Punta San Pancrazio

The coast from Carta Romana to Punta della Pisciazza shows a complex pyroclastic sequence with interbedded lava flows which is composed of Carta Romana Pyroclastics at the base and Casa Mormile and Piano Liguori Pyroclastics at the top. Doubled

Fig. 12 - Views from South (a) and North (b) of Ischia Castle Lava Dome (~ 130 ka).



Punta della Pisciazza, the base of the exposed sequence is composed of lavas dated at 73 ka (Lave di Parata, Vezzoli, 1988).

At Grotta del Mago, a deep natural cave consisting of several chambers of various size, the following sequence is shown (Fig. 13): Lave di Parata (A, Fig. 13) at the base, mantled by the plinian pyroclastic fallout and flow complex sequence of Formazione di Pignatiello (B, Fig. 13) which is an important regional theprostratigraphic marker. The sequence continues with the Plinian pyroclastic-fallout and -surge deposit of Secca d'Ischia (C, 61 ka; Fig. 13), which likely was emitted by a vent now located into the sea between Ischia and

Procida island. At the top the Piano Liguori Pyroclastics (E, Fig. 13) close the sequence. In correspondence of the cave the darkish deposits of Grotta del Mago scoria cone (D, 28 ka; Fig. 13) are well visible, as well as its feeding dyke that lies along a NW-SE trending eruptive fracture.

At Punta San Pancrazio the homonymous greyish-black lavas are exposed, likely representing a portion of an eroded lava dome, originated a little further to the south (Sbrana and Toccaceli, 2011).

### Stop 1.5: From Punta San Pancrazio to Punta della Signora

From the western edge of Punta San Pancrazio towards west, the scene is morphologically dominated by Mt. Vezi (Fig. 14) and, in correspondence of the San Pancrazio Beach, the sequence of the exposed deposits is



Fig. 13 - Grotta del Mago succession (dotted lines = limits between volcanic units). A = Lave di Parata (73 ka), B = Formazione di Pignatiello, C = Secca d'Ischia Pyroclastics (61 ka), D = Grotta del Mago Scoria (28 ka), E = Piano Liguori Pyroclastics (5.5 ka).



characterized, at the base, by the yellowish, highly fractured, pyroclastic-current deposits of the Upper Member of Scarrupata di Barano Tuffs (A, Fig. 14). These tuffs are the remnants of a series of old (>150 ka) volcanic edifices (tuff-cones) that form the backbone of the south-eastern part of the island, built during an intense early magmatic and hydromagmatic activity. They are covered by the greyish-black scoria spatters of Mt. Vezzi (B, 126 ka; Fig. 14) representing the product of lava fountaining along eruptive fractures in the south-eastern sector of Ischia.

The high cliff of Scarrupata di Barano shows at base the complete sequence of the Scarrupata di Barano Tuffs, which reaches a thickness of more than 100 m. At the western edge of the bay, the 220 m thick deposit of La Guardiola Lavas is made of darkish lavas and scoria beds, produced by low-energy Strombolian explosions and lava fountaining activity. It is mantled by the Piano Liguori Pyroclastics (5.5 ka).

Towards west the Scarrupata di Barano is separated from the Maronti beach by the Punta della Signora and Capo Grosso promontories.

At Punta della Signora, a 50 m thick sequence of welded spatters (Fig. 15, A; Punta della Signora Spatters, 147 ka) crops out at the base. The spatters are overlain by the deposits of the Scarrupata di Barano Tuffs and the Lower Member of Secca d'Ischia Pyroclastics (C, Fig. 15). Monte Cotto Tuffs (D, 38 ka; Fig. 15) and Piano Liguori Pyroclastics (E, Fig. 15) close the sequence at the top. Between Punta della Signora and Capo Grosso a N-S trending vertical fault defines the contact between the oldest dated deposits of Punta della Signora Spatters (A; 147 ka, Fig. 15; Vezzoli, 1988) and the



Fig. 14 - The San Pancrazio beach succession (dotted white lines = limits between volcanic units; red lines = faults). A = Upper Member of Scarrupata di Barano Tuffs (>150 ka), B = Mt. Vezzi welded scoria (126 ka), C = Punta San Pancrazio Lavas, D = Lower Member of Formazione di Pignatiello, E = San Pancrazio Beach Tuffs, F = Lower Member of Secca d'Ischia Pyroclastics (61 ka), G = Piano Liguori Pyroclastics (5.5 ka).

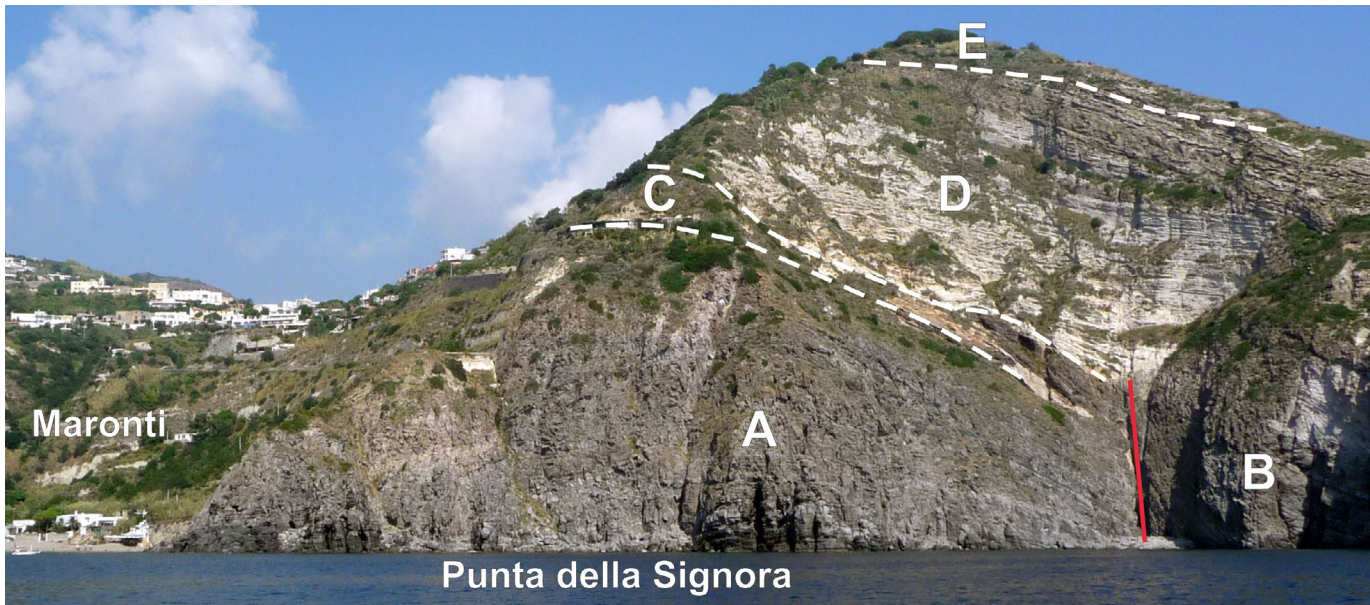


Fig. 15 - Punta della Signora sequence (dotted white lines = limits between volcanic units; red line = fault). A = Punta della Signora Spatters (147 ka), B = Capo Grosso welded Scoria, C = Scarrupata di Barano Tuffs + Lower Member of Secca d'Ischia Pyroclastics (61 ka), D = Monte Cotto Tuffs (38 ka), E = Piano Liguori Pyroclastics (5.5 ka).

Capo Grosso welded Scoriae (B, Fig. 15).

### Stop 1.6: Maronti beach and Mt. Epomeo southern slope

The Maronti beach was the widest beach of the Ischia island in the past. Nowadays, due to the shore erosion and the anthropic activity, its extents are strongly reduced. Along the beach numerous thermal springs are noticeable, whereas in the western side, close to S. Angelo, some high temperature fumaroles ( $\sim 100^{\circ}\text{C}$ ) are known. The deposits outcropping at the base of Mt. Epomeo southern slope are mainly debris-avalanche

deposits containing heterometric greenish to light-grey blocks of hydrothermalized tuffs and epiclastic deposits due to the reworking of intra-calderic deposits during the uplift of Mt. Epomeo block. Subordinate debris-flow deposits, produced by the remobilization of the aforesaid deposits, outcrop in the same area. Along the slope of Mt. Epomeo at least three orders of marine terraces can be viewed. They represent different phases of uplift of the resurgent Mt. Epomeo block.

In the submerged counterpart of this basin, an extensive long-range side scan sonar survey, evidenced the presence of a huge debris avalanche deposit. The so-called "Ischia Debris Avalanche - IDA" has been recognized as the largest event of this type described at Ischia (Chiocci and de Alteriis, 2006; de Alteriis and Violante, 2009; Fig. 16), covering an area of 250-300 km<sup>2</sup>, extending from the foot of the submarine escarpment (-550 m to -1100 m and with a runout of 50 km). Tibaldi and Vezzoli (1998, 2004) associated the avalanche events to the recurrent collapse of the southern flank of Mount Epomeo, due to phases of acceleration of the resurgence

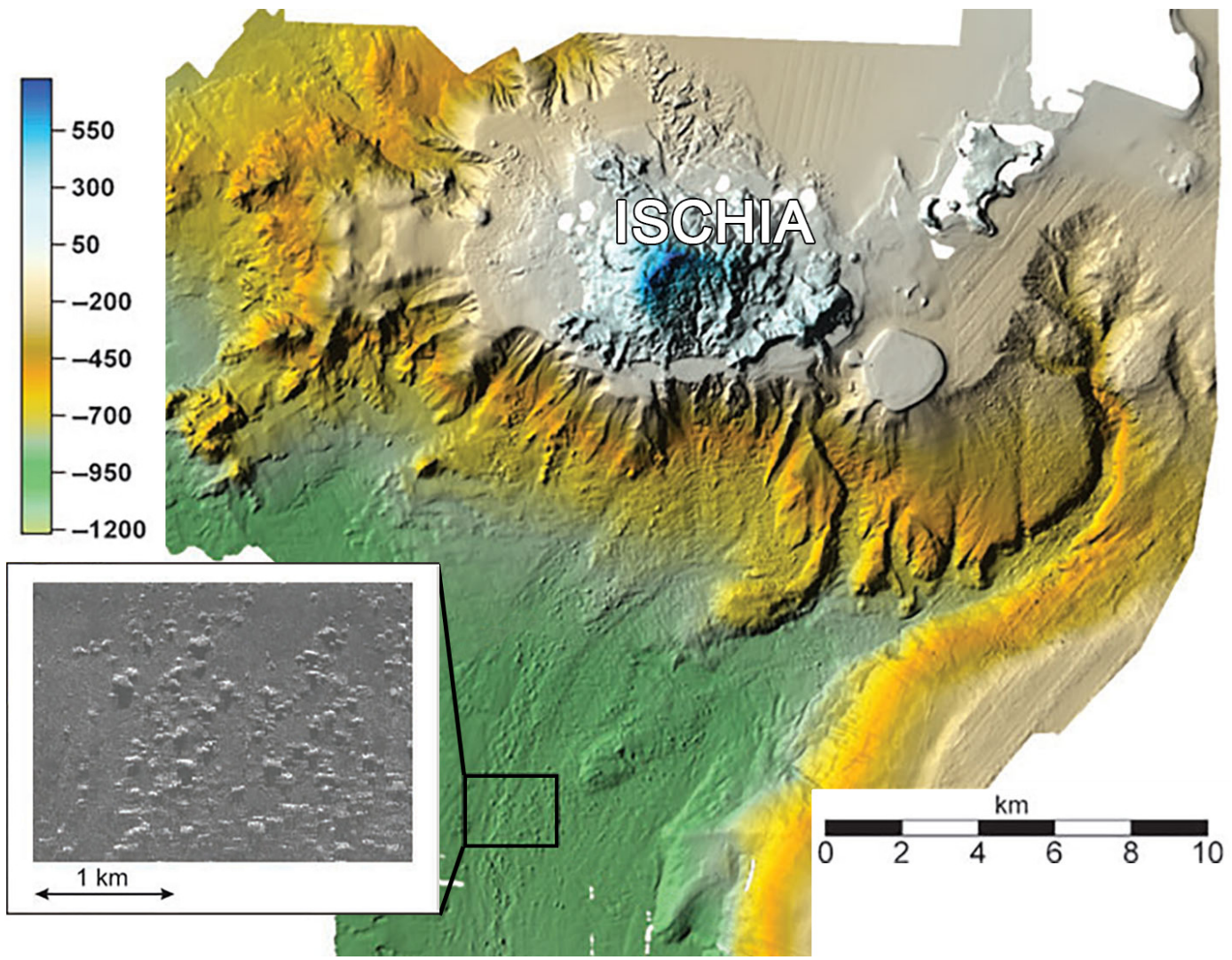


Fig. 16 – Digital Terrain Model of Ischia offshore. The multibeam surveys denoted the presence of hundred metres large blocks at about 18 km from the source area (low frequency side scan sonar image in the box) and at 950 m depth (modified after Chiocci et al., 2006).

(uplift rates up to 3 cm/yr), and identified three main mechanisms that may have contributed to an intermittent increase of the shear stress along the slopes in the last 33 ka: i) the uplift driven by the rising of magma which produces an increase in the static load; ii) the fault-associated tilting; iii) the earthquake shaking. Due to contrasting stratigraphic evidence and age determinations, the volume, timing and dynamics of emplacement of IDA (single event or multi-event) are still uncertain.

**Stop 1.7: Sant'Angelo and Sorgeto**

The western end of the Maronti beach is defined by the small promontory of Sant'Angelo. It is connected to the coast through a narrow isthmus and hosts the ruins of an Aragonese tower at its top. The Sant'Angelo promontory is the remnant of a lava dome, which was truncated by an E-W trending fault that lowered the northern side of the dome. This is in turn mantled by a pyroclastic sequence (Fig. 17). At the base of the sequence the Mt.

<https://doi.org/10.3301/GFT.2018.03>



Sant'Angelo scoriaceous grey lavas (A, ~100 ka, Fig. 17; Vezzoli, 1988) are exposed. They are overlain by the Elephant Pyroclastics (~97 ka; Sbrana and Toccaceli, 2011) that lies above a marine erosional surface. The Elephant Pyroclastics are a succession of pumice-fallout beds and fine-graded pyroclastic-current layers (B, Fig. 17). The sequence continues to the top with a lithic-rich breccia deposit (C, Punta Sant'Angelo Breccia; Fig. 17), which has been considered in the past the basal breccia of the Mt. Epomeo Green Tuff eruption.

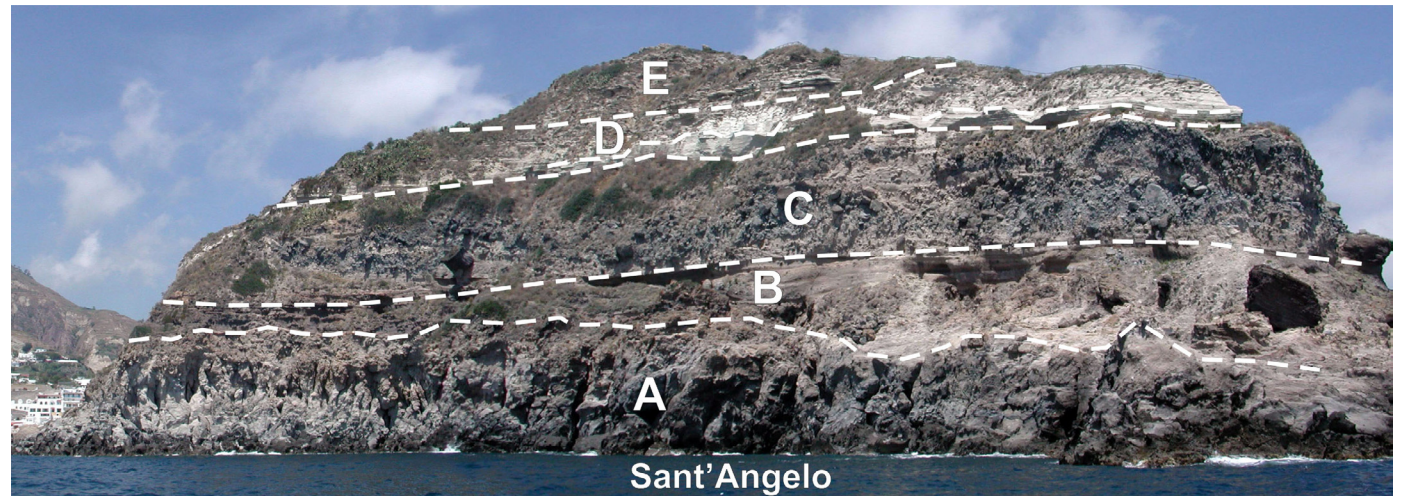


Fig. 17 – S-E view of Sant'Angelo promontory (dotted lines = limits between volcanic units). A = Mt. Sant'Angelo Lavas (~100 ka), B = Elephant Pyroclastics (~97 ka), C = Punta Sant'Angelo Breccia, D = San Michele Tuffs, E = Sant'Angelo Tuffs (~20 ka).

The San Michele Tuffs, a hydromagmatic deposit likely originated from a tuff cone located in the offshore south of Maronti, and the overlying Sant'Angelo Tuffs (E, ~20 ka; Fig. 17) close the sequence. The Sant'Angelo Tuffs are a thinly stratified succession composed of a basal yellowish tuff breccia, overlain by pyroclastic surge beds with bomb-sags, ash and pumice lapilli fallout layers, massive coarse pyroclastic density current deposits and an upper pumice- and scoria-bomb fallout deposit at the top. These tuffs outcrop along the coast between Sant'Angelo and Punta Chiarito and represent the product of a tuff-cone forming eruption, whose vent was likely located originated from a tuff cone located in the near offshore to the south-east of Punta Chiarito in the sea, as also evidenced by bathymetric data (Sbrana and Toccaceli, 2011).

The coast from Sant'Angelo to Punta Chiarito is characterized by a 50 m high cliffs with hanging valleys, cut within the Sant'Angelo Tuffs deposits.

A picture of Baia di Sorgeto, whose hydrothermal springs (80-90°C) at sea level give the opportunity to swim also in winter time, is reported in Fig. 18. In the eastern part of the bay, the highly fractured Punta Chiarito Lavas (A, Fig. 18) are part of a lava dome cut by a fault, which lowered its northern side. The lavas are overlain by the Sant'Angelo Tuffs (G, Fig. 18) and by patches of a mud-flow deposit (H, Fig. 18), widely distributed in



the Succhivo area. This mud-flow deposit also overlies the pyroclastic deposit of Punta Chiarito Thepra, which buried a Greek settlement of the 8<sup>th</sup>-7<sup>th</sup> century B.C., as it was evidenced in the archaeological excavations on the top of Punta Chiarito promontory (Gialanella, 1998; de Vita et al., 2006).

In the middle of the bay, a normal fault (red line, Fig. 18) displaces towards south the Sorgeto Tuffs (C, Fig. 18), putting them in contact with the Sant'Angelo Tuffs (G, Fig. 18). The Sorgeto Tuffs are a succession of hydromagmatic pyroclastic-fall and -flow deposits, belonging to the Ancient Ischia Synthem (Sbrana and Toccaceli, 2011). Along this fault the hyperthermal spring of Sorgeto emerges with its chlorinated-alkaline waters.

In the western part of the Sorgeto bay the altered and highly fractured lavas of Capo Negro (B, Fig. 18) are at the base of the succession. The lavas are overlain by the Sorgeto Tuffs (C, Fig. 18) and by the Cava Pelara Pyroclastics (D, Fig. 18), a succession of spatter- and breccia- fallout deposit, capped by yellowish stratified tuffs at the top.

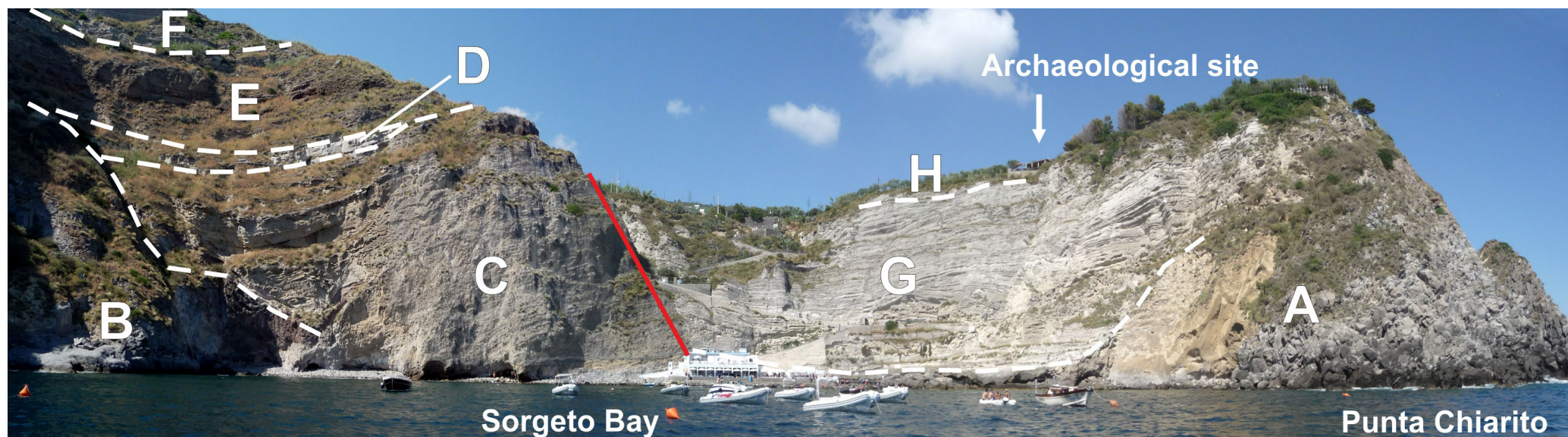


Fig. 18 - Sorgeto Bay (dotted white lines = limits between volcanic units; red line = fault). A = Punta Chiarito Lavas, B = Capo Negro Lavas, C = Sorgeto Tuffs, D = Cava Pelara Pyroclastics, E = Scarrupo di Panza Pyroclastics, F = Russo Pyroclastics, G = Sant'Angelo Tuffs (~20 ka), H = mud Flow. The archaeological site hosts the rests of a Greek settlement dated VIII-VII century BC which was buried by the deposits of Punta Chiarito eruption.



The sequence continues towards the top with the Scarrupo di Panza Pyroclastics (E, Fig. 18), consisting of reddish to dark-grey scoriaceous lapilli-fallout deposit, which likely originated from a vent located in the sea close to La Nave rock. The Russo Pyroclastics (F, Fig. 18) closes the sequence. This deposit consists of a succession of grey pumice-fallout beds, related to three Plinian eruptions, produced by vents located in the offshore of Punta Imperatore (Sbrana and Toccaceli, 2011).

### Stop 1.8: From Capo Negro to Punta Imperatore

Towards west the coast beyond Capo Negro is dominated by the units belonging to the Campotese Subsynthem (Sbrana and Toccaceli, 2011), with the darkish scoriaceous lavas of Pilaro, whose thickness reaches about 100 m, outcropping at the base of the exposed sequence. These lavas are overlain by the Scarrupo di Panza and Russo Pyroclastics, up to Grotta del Mavone, where a normal fault lowered towards west the Pilaro Lavas and put them in contact with a small lava flow (Rosicariello Lavas). At Grotta del Mavone the highly porphyric homonymous lavas (A, ~29 ka, Fig. 19; Vezzoli, 1988) are at the base of the succession that ends at the top with the Scarrupo di Panza Pyroclastics (B1-2, Fig. 19). This last deposit is widely exposed along the cliff up to Punta Imperatore, and the dark welded-scoria beds of the upper member (B2, Fig. 19) thicken in this direction due to the proximity to the emission vent. At Punta dello Schiavo the light-grey lavas of Pomicione lava-dome (C, Fig. 19) cover the Scarrupo di Panza Pyroclastics at the top of the succession.

The volcanic sequence at Punta Imperatore is reported in Fig. 20. At the base the light-grey Punta Imperatore Lavas (A, ~117 ka; Vezzoli, 1988) are characterized by an erosional marine surface with

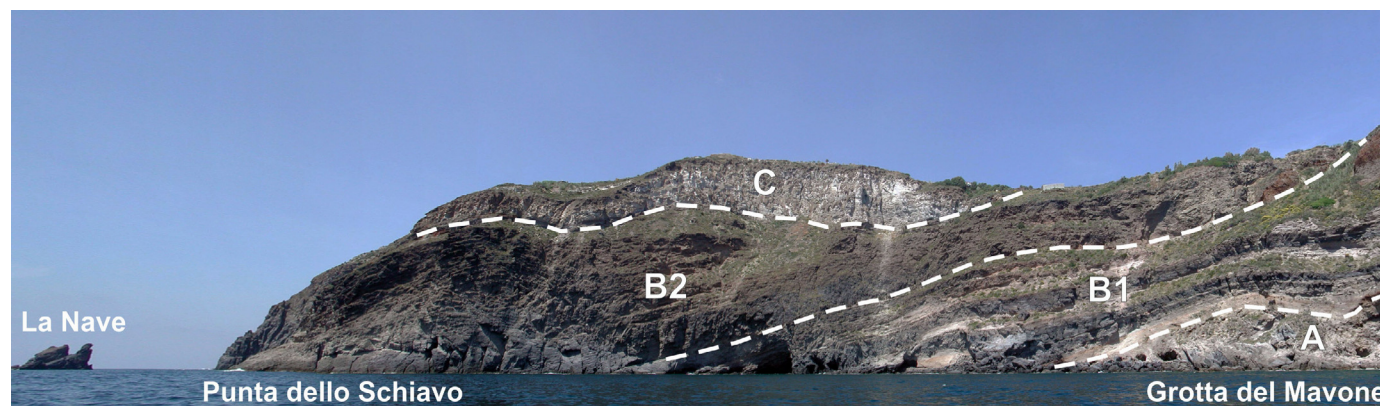


Fig. 19 – Coast between Grotta del Mavone and Punta dello Schiavo (dotted white lines = limits between volcanic units). A = Grotta del Mavone Lavas (~ 29 ka), B (1-2) = Lower Member (1) and Upper Member (2) of Scarrupo di Panza Pyroclastics, C = Pomicione Lavas. La Nave rock represents likely the rests of eruptive centre which originated the Scarrupo di Panza Pyroclastics.



patches of fossiliferous sands. The sequence continues with different pyroclastic deposits, dated between 98 and 18 ka, separated by paleosols and erosional surfaces. These deposits vary from very proximal breccia and scoria to fine-graded tuffs, and were emitted by local vents and vents located in the Punta Imperatore offshore.

### Stop 1.9: The Forio area and the western slope of Mt. Epomeo

The coast between Punta Imperatore and Forio is well-known for the Citara beach and its hot-springs, which is the site of one of the most famous thermal park of the island (Fig. 21a). Along the coast, between Punta Imperatore and Pietre Rosse, the Citara Tuffs (~33 ka; Vezzoli, 1988) outcrop, showing high-angle unconformities and paleo-valleys filling, with spectacular slumping structures and soft deformations in the pyroclastic-currents deposits (Fig. 21b).

The Citara Tuffs are a succession of yellowish stratified pyroclastic-current deposits with accretionary lapilli, diffuse cross-bedding structures and bomb sags, which likely were emitted by tuff-cones in the off-shore of Citara. This succession is overlain in the Citara and Forio area by rock-avalanche (4th century B.C.; Della Seta et al., 2012) and debris-flows deposits (Della Seta et al. 2012; Di Martire et al., 2012) with several hummocks emerging from the sea. Also the coast between Forio and Zaro is dominated by these rock-avalanche deposits with

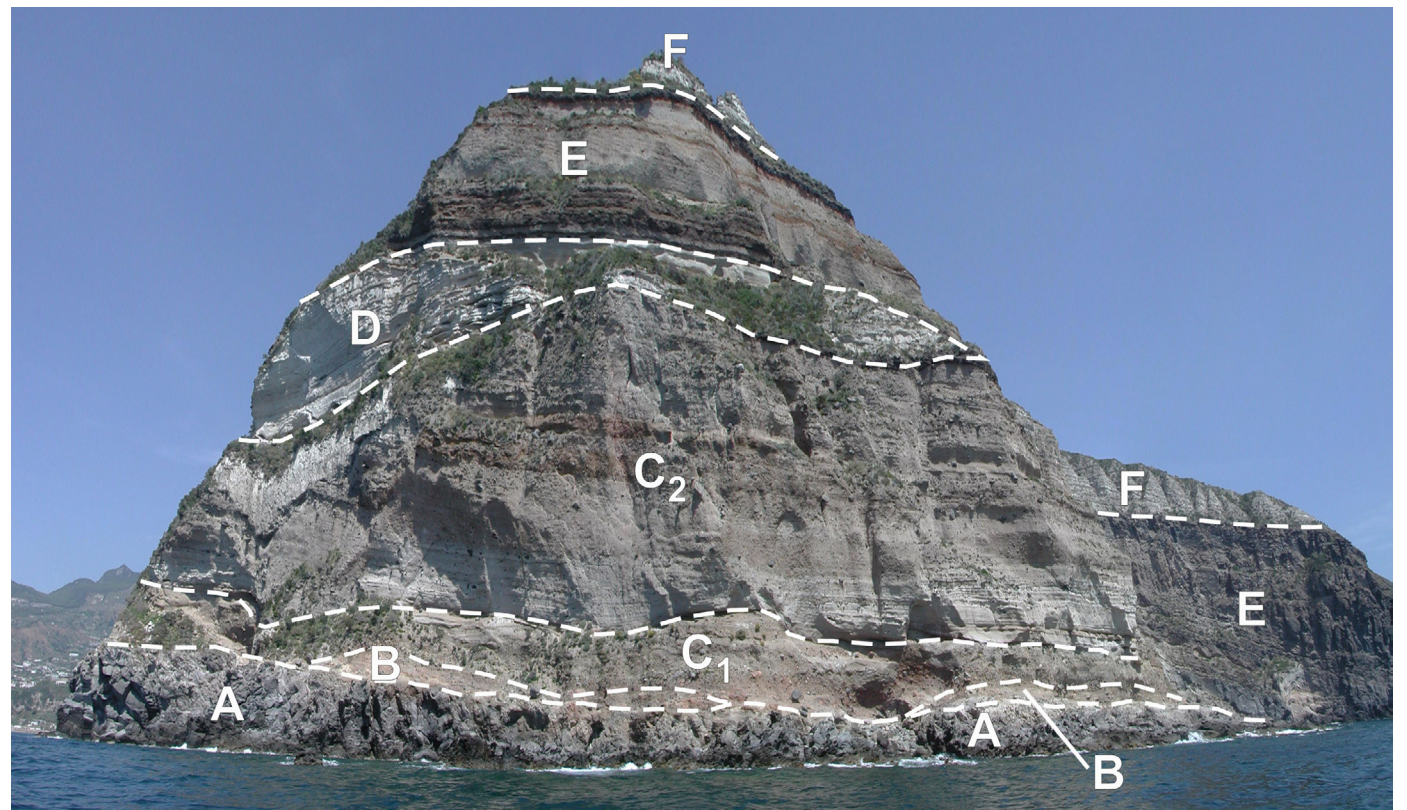


Fig. 20 – Sequence at Punta Imperatore promontory (dotted white lines = limits between volcanic units). A = Punta Imperatore Lavas (~117 ka), B = Elephant Pyroclasts (~97 ka), C = Spiaggia di Agnone Pyroclastics (C1 = lower member, C2 = upper member), D = Citara Tuffs (~45 ka), E = Scarrupo di Panza Pyroclastics, F = Faro Punta Imperatore Pyroclastics (~18 ka).



Fig. 21 – Citara beach with Citara Tuffs deposits (~ 33 ka) at the back of the thermal park (a) and spectacular slumping and soft deformation structures in Citara Tuffs pyroclastic currents (b).

numerous hummocks distributed in the near off-shore of Forio, up to the San Francesco beach. The western flank of Mt. Epomeo is clearly visible from this part of the coast, with its steep slopes, generated by high-angle vertical-to-reverse faults related to the resurgence, and the slope-instability related deposits. The Mt. Nuovo DSGSD block is well evident as well in the western part of the landscape, at the foot of the Falanga hanging wall. The morphological evolution of these slopes and the characteristics of the related deposits, will be outlined during the second day of this field trip.

**Stop 1.10: From Zaro promontory to Mt. Vico**

The Zaro promontory is a lava field, formed by the products of several



Fig. 22 – Zaro Lavas outcrop (basal flow, ~ 6 ka) at San Francesco beach.



effusive and low-energy explosive eruptions that generated lava domes, lava flows and scoria-fallout deposits at around 6 ka (Vezzoli, 1988; Fig. 3). These products were erupted from a fissure-vent area, along NE-SW trending fractures that likely reactivated regional faults, also active during the formation of the caldera and the following resurgence. These faults also mark the limit of the resurgent area in the north-western corner of the caldera (de Vita et al., 2010). Between Zaro and Mt. Vico the bay of San Montano was the site of the first landing in southern Italy of Greek colonies from Euboea in the 8<sup>th</sup> century BC. The Greek colony of Pithekoussai included an *acropolis*, on top of Mt. Vico, a *necropolis* with more than 2,000 graves in the San Montano valley, and a *chora* that likely extended from Mezzavia (between Lacco Ameno and Forio) to the southern coast of the island.

The Mt. Vico promontory, east of San Montano Bay, is a lava dome (A, 75 ka, Fig. 23; Vezzoli, 1988) displaced by NW-SE and NE-SW trending faults, which are the site of fumarole activity and several hot thermal springs. The lava dome is overlain by a sequence of pyroclastic deposits composed of pumice lapilli beds (Pignatiello Formation; B, Fig. 23), a breccia belonging to the Porticello formation (C, Fig. 23), a stratified succession of whitish fine ash and pumice beds belonging to the Secca d'Ischia Pyroclastics (D, Fig. 23) (Sbrana and Toccaceli, 2011). At the top of the sequence a stratified ash- and pumice lapilli-deposit has been correlated to the Cretaio Tephra (E, Fig. 23), which is the deposit of the highest-magnitude eruption occurred during the past 10 ka, from a vent located in the eastern part of the island (1<sup>st</sup> century BC - 1<sup>st</sup> century AD; Orsi et al., 1992).

The Mt. Vico promontory, east of San Montano Bay, is a lava dome (A, 75 ka, Fig. 23; Vezzoli, 1988) displaced by NW-SE and NE-SW trending faults, which are the site of fumarole activity and several hot thermal springs. The lava dome is overlain by a sequence of pyroclastic deposits composed of pumice lapilli beds (Pignatiello Formation; B, Fig. 23), a breccia belonging to the Porticello formation (C, Fig. 23), a stratified succession of whitish fine ash and pumice beds belonging to the Secca d'Ischia Pyroclastics (D, Fig. 23) (Sbrana and Toccaceli, 2011). At the top of the sequence a stratified ash- and pumice lapilli-deposit has been correlated to the Cretaio Tephra (E, Fig. 23), which is the deposit of the highest-magnitude eruption occurred during the past 10 ka, from a vent located in the eastern part of the island (1<sup>st</sup> century BC - 1<sup>st</sup> century AD; Orsi et al., 1992).

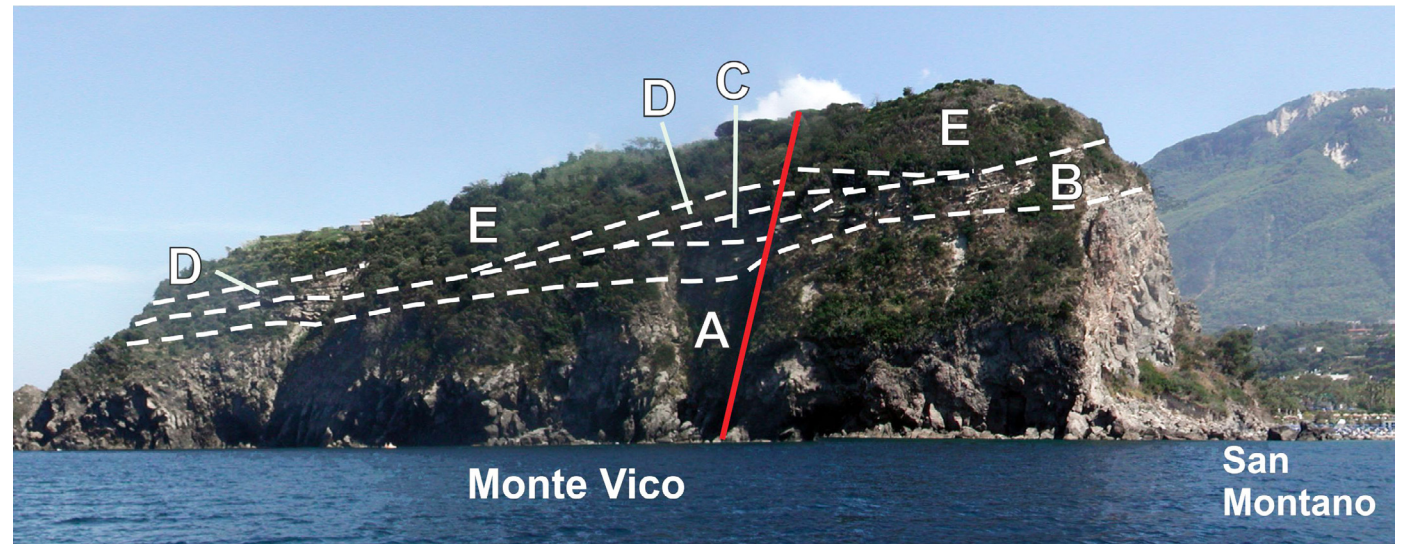


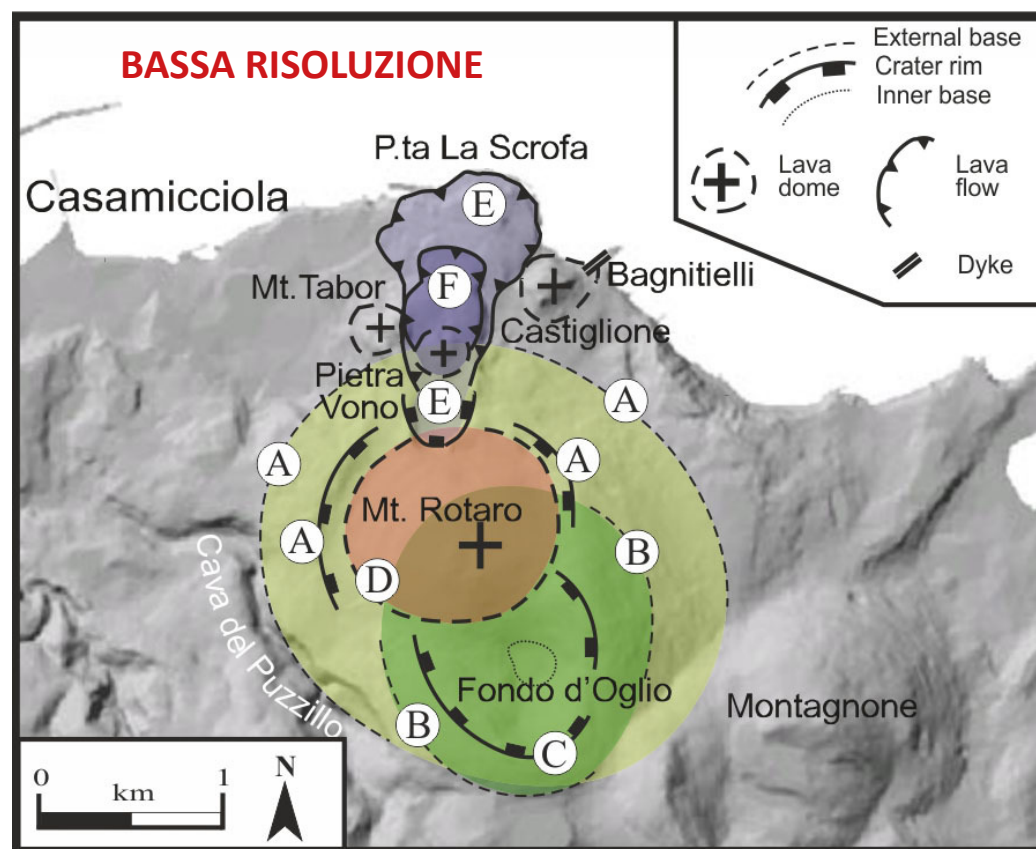
Fig. 23 – Northern slope of Mt. Vico (dotted white lines = limits between volcanic units; red line = fault). From base to top: A = Mt. Vico Lavas (75 ka), B = Pignatiello Formation, C = Il Porticello Breccia, D = Secca d'Ischia Pyroclastics, E = Cretaio Tephra (1<sup>st</sup> century BC – 1<sup>st</sup> century AD).



## 2<sup>nd</sup> day - Recent volcanic activity at Ischia

### Stop 2.1: The Rotaro volcanic complex (40°44''25.30'N; 13°55''11.50'E)

The Rotaro volcanic complex is one of the few examples of polygenic volcanoes at Ischia, activated in the last 10 ka of volcanism. Its morphology is clearly visible from Casamicciola town, looking towards east. The volcanic edifice is grown-up during at least nine explosive and effusive eruptive phases with vent migration towards north along a N-S trending fault active since at least 8.5 ka (Fig. 24). The first eruptive phase created a pumice cone (A, Fig. 24) as testified by the pyroclastic sequence of Puzzillo Tephra (de Vita et al., 2010), exposed in the valley to the south-west of the edifice (Cava del Puzzillo), where it reaches a thickness of about 50 m. This sequence is composed of at least three units, separated by paleosols and erosional surfaces: the oldest one overlies a fossiliferous marine silt deposit dated 8.5 ka (Buchner et al., 1996); the youngest is dated at around 6.2 ka (Puzzillo Tuffs, Sbrana and Toccaceli, 2011).



The basal sequence is a proximal deposit of massive pumice and scoria fallout, intercalated with subordinate, cross-laminated to plane-parallel ash-surge beds. The intermediate sequence is mainly composed of ash-surge deposits, with large- and small-scale cross-lamination, and subordinate massive pumice-fallout beds, containing abundant lithic fragments (Fig. 25a). Several bomb sags, suggests direction of ballistic clasts from the eastern quadrants (Fig. 25b). The

Figure 24 is a sketch map of the Rotaro volcanic complex. It shows the complex's evolution with features labeled A through F. A legend in the top right corner defines the symbols: External base (dashed line), Crater rim (solid line), Inner base (dotted line), Lava dome (circle with a cross), Lava flow (curved arrow), and Dyke (double line). The map includes labels for Casamicciola, P.ta La Scrofa, Mt. Tabor, Pietra Vono, Cava del Puzzillo, Fondo d'Oglio, Montagnone, Bagnitielli, and Castiglione. A scale bar (0-1 km) and a north arrow are in the bottom left.

Fig. 24 - Sketch of morphologically evident features related to the Rotaro volcanic complex evolution. A = edifice generated by, Puzzillo Piroclastics; B = Bosco della Maddalena lava dome; C = Fondo d'Oglio Tephra crater; D = Mt. Rotaro lava dome; E = Punta La Scrofa lava flow; F = Pietra Vono lava flow and spine.



sequence at the top is composed of stratified, pumice-fallout beds, with interbedded discontinuous scoria-fallout beds, containing scattered dense glass clasts.

The following phase produced a lava dome in correspondence of the area of Bosco della Maddalena (B, Fig. 24). These lavas are exposed within the Fondo d'Oglio crater and along the eastern slopes of the Cava del Puzzillo valley. The lava dome was partially dismantled by the subsequent Strombolian activity, which generated the Fondo d'Oglio crater (C, Fig. 24e). The products of this activity are mainly composed of black, well vesiculated, locally welded scoria-fallout beds and subordinate lensoid beds of dark angular pumice and lithic fragments. This deposit overlies a paleosol developed above the Bosco della Maddalena lavas (Fig. 26a). The presence of a paleosol over the lavas testifies a pause of the Rotaro volcanic activity before the eruption of Fondo d'Oglio Tephra. A good exposure of this deposit is visible at the beginning of the road that leads inside the Fondo d'Oglio crater where the pyroclastic deposit of Bosco della Maddalena Tephra overlies the Fondo d'Oglio Tephra (Fig. 26a). The Bosco della Maddalena Tephra represents a new phase of the Rotaro volcanic activity, whose products are mainly exposed inside the crater of Fondo d'Oglio. These products consist of a succession of fine-to-coarse fallout beds and subordinate coarse ash-surge beds likely originated from a

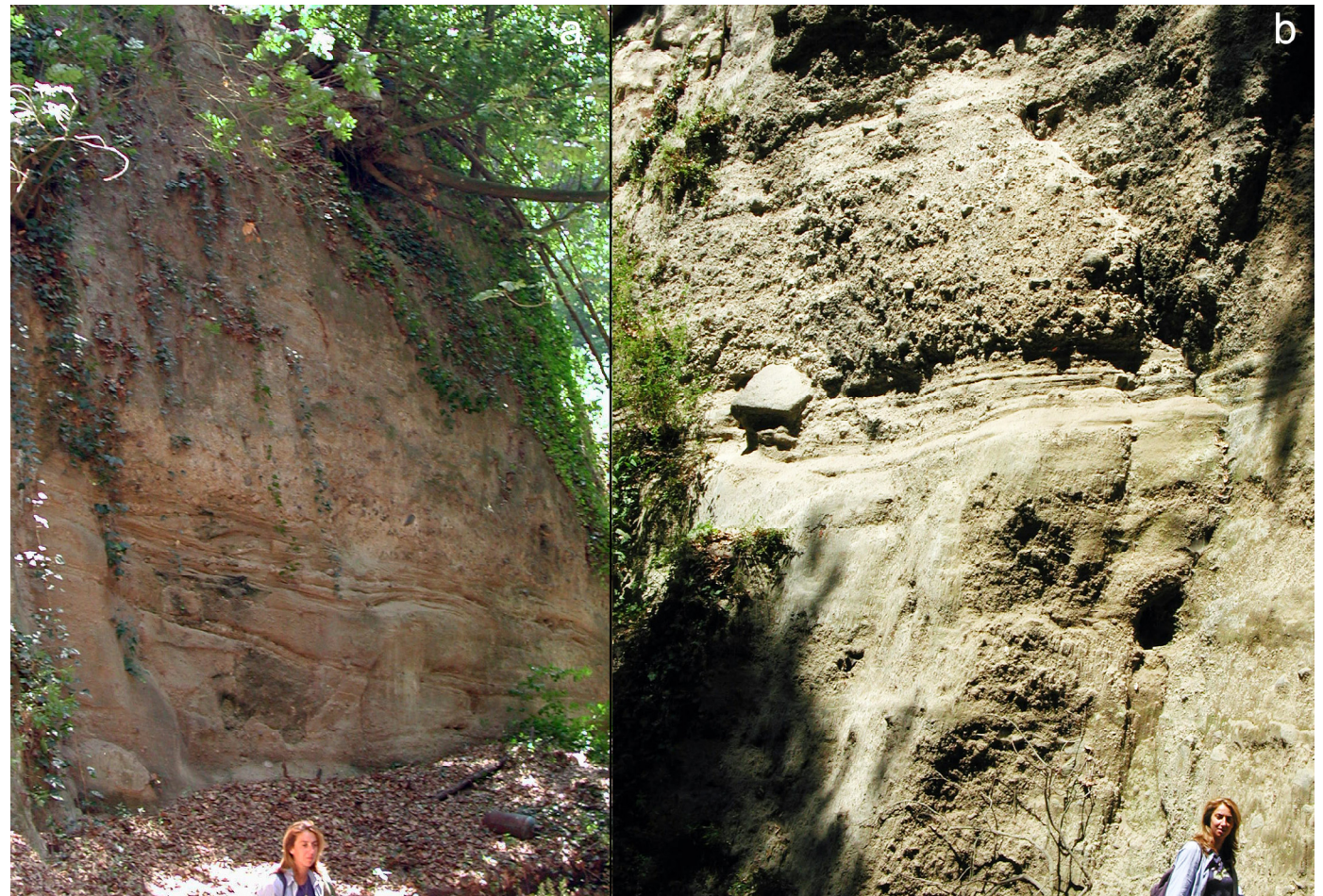


Fig. 25 – Outcrops of Puzzillo Tephra in the locality Cava del Puzzillo; a) intermediate sequence; b) detail of bomb-sag.

of a succession of fine-to-coarse fallout beds and subordinate coarse ash-surge beds likely originated from a



low-magnitude eruption characterized by a pulsating and continuously collapsing eruption column that did not allow the formation of a cone and took place from a vent located northwest of the previous one (Fig. 26b). Shortly afterward, a new lava dome (Mt. Rotaro Lava Dome, D in Fig. 24) was emitted in correspondence of the new crater. Locally, the well vesiculated and scoriaceous lavas of the dome are foliated along subvertical planes and are characterized by fluidal texture. The last phases of the Rotaro Volcanic complex are characterized by the emission of two lava flow, Punta La Scrofa (E, Fig. 24) and Pietra Vono (F, Fig. 24) Lavas. These units were

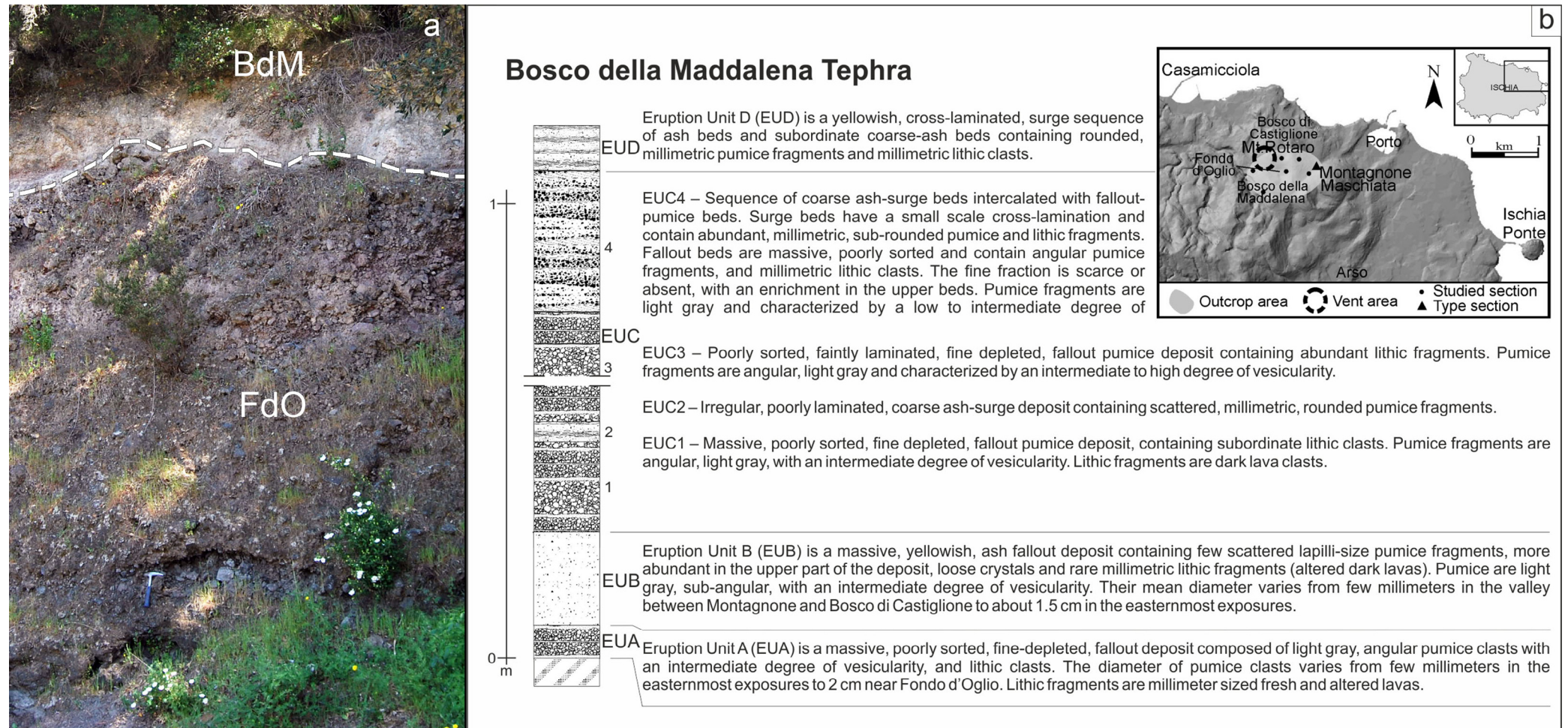


Fig. 26 – Outcrop of Fondo d’Oglio Tephra and basal beds of Bosco della Maddalena Tephra (a) at the crossroad to the Fondo d’Oglio crater; b) reconstruction of Bosco della Maddalena Tephra deposits and outcrop area (modified after de Vita et al., 2010).



erupted from vents that progressively migrated towards north, along a N-S trending fissure. The upper part of Punta La Scrofa lava flow is exposed along the northern coast of the island, where the scoriaceous flow-front is affected by continuous rock-falling. The internal part of the lava body is generally massive and porphyritic, from light to dark grey in colour and is well exposed along the road from Casamicciola to Castiglione. The Pietra Vono lava flow is exposed in the homonymous locality and its emplacement was followed by the extrusion of a very viscous spine of lava (de Vita et al., 2010).

## **Stop 2.2: The Montagnone-Maschiata volcanic complex and the deposits of recent volcanic activity (last 10 ky; 40°44"07.20'N; 13°55"22.60'E)**

The road connecting Mt. Rotaro to the Cretaio locality passes through several deposits and volcanic landforms, produced during the last 10 ka of activity. Close to the south-eastern Mt. Rotaro slopes another example of polygenic volcano is visible: the Montagnone-Maschiata volcanic complex (Fig. 27a). It is a composite volcano formed during several explosive and effusive eruptions separated by quiescence phases of variable length. The first eruptive phases began in the 5th century BC and produced a lava dome and a lava flow that flowed northward, reaching the coast close to Ischia Porto (de Vita et al., 2010). Subsequently the lava dome was partially destroyed by at least three explosive eruptions. The first explosive eruption produced the Posta Lubrano pyroclastic deposit, a succession of yellowish ash-surge and ash-fallout beds with intercalated pumice lapilli-fallout beds (Fig. 27b). The Cretaio Tephra, generated by the following activity, is the products of the highest magnitude eruption of the last 10 ka activity (Orsi et al., 1992) which took place between the 1<sup>st</sup> century BC and 1<sup>st</sup> century AD.

At Cretaio locality several outcrops of the Cretaio Tephra are visible (Fig. 27c). The Cretaio Tephra eruption started with a phreatomagmatic phase that produced base surges. Then a pulsating sub-Plinian to Plinian eruption column generated widely dispersed pumice-fallout deposits over a wide area in the eastern part of the island. A partial collapse of the column generated pyroclastic surges during this phase. A fine-grained surge deposits, followed by a final sub-Plinian sequence of pumice-fallout deposits close the eruption sequence.

After the Cretaio eruption a new crater formed in the Montagnone-Maschiata composite cone, due to the Bosco dei Conti Tephra eruption (1.4 ka; Orsi et al., 1996; de Vita et al., 2010), whose deposit overlies a thin paleosol developed above the Cretaio Tephra.

The Bosco dei Conti Tephra eruption started with a sub-Plinian explosion that generated a pulsating eruption column, from which a basal fallout deposit was formed and dispersed south-eastward. Then

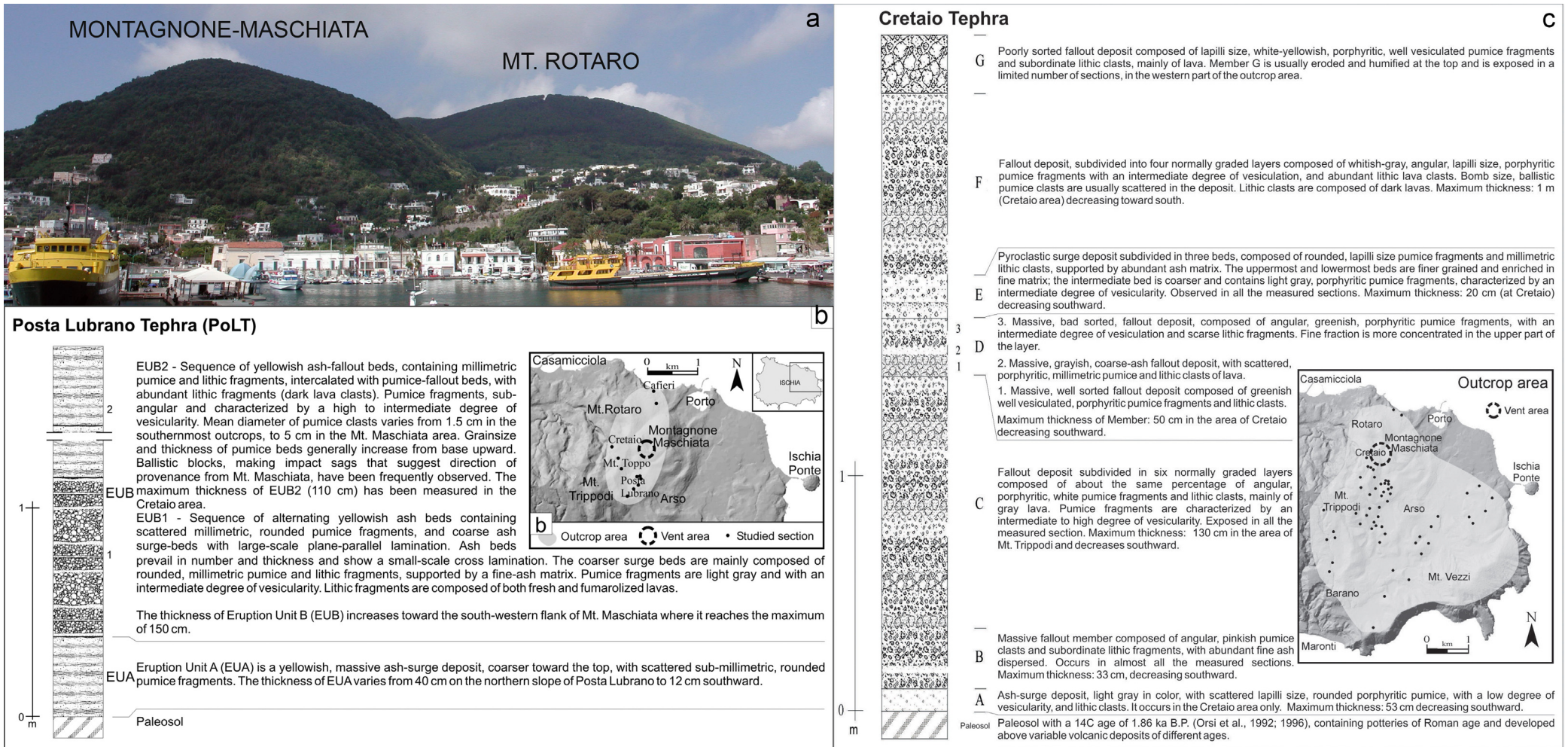


Fig. 27 – A view from Ischia harbour of northern slopes of Montagnone-Maschiata and Mt. Rotaro (a). Reconstructions of Posta Lubrano Tephra (b) and Cretaio Tephra (c) deposits and the outcrop areas (modified after de Vita et al., 2010).

the eruption changed to alternating phreatomagmatic and magmatic phases that originated a sequence of pyroclastic-surge and -flow deposits, intercalated with subplinian-to-Strombolian fallout beds. The final stages of this eruption were characterized by a renewed increase in the mass eruption rate and the formation of a pulsating sub-Plinian eruption column, in which the particles were more fragmented, suggesting an efficient water/magma interaction. The last phases of Montagnone-Maschiata volcano



produced the Maschiata lava dome, which during a final deflation emitted two small lava flows from the base of its southern slope.

Passed the Cretaio locality, following the road to L'Arso towards south-east, a sequence of pyroclastic deposits outcrops along the slope of Mt Toppo, a lava dome truncated by a NW-SE trending normal fault, which downthrown the north-eastern flank of the dome. The sequence of pyroclastic deposits includes the Cava Bianca Tephra at the base and the Posta Lubrano, Cretaio and Bosco dei Conti Tephra towards the top (de Vita et al., 2010). The Cava Bianca Tephra eruption occurred in the 4<sup>th</sup> century BC (Civetta et al., 1999), was initially phreatomagmatic, with the formation of thin pyroclastic-surge-deposits, but very soon it turned magmatic with the formation of a low, sub-plinian eruption column, which produced poorly sorted and weakly dispersed fallout deposits. The eruption ended with a new phreatomagmatic phase that generated thin pyroclastic-surge deposits of very limited areal extent (de Vita et al., 2010).

### Stop 2.3: The Arso crater (40°43'45.00'N; 13°56'02.50'E)

The Arso volcanic centre activated at the intersection of NW-SE and NE-SW trending faults system. The eruption was the last one of Ischia island and begun in 1302 A.D. with a strombolian phase which built a



Fig. 28 - View from L'Arso crater to Punta Molina, including Castello d'Ischia. The dotted yellow line is the border of L'Arso lava flow erupted in 1302 AD (courtesy Google Earth).



small asymmetric scoria cone due to the accumulation of fallout spatters over a rough paleo-morphology. The following phase produced a lava flow which proceeded towards north-east, reaching the sea at Punta Molina. Notwithstanding the current heavy urbanization, it is still possible to identify the lava flow morphology (Figs 3, 11, and 28). Inside the Arso crater both the lava blocks and scoria deposits are well exposed, forming pinnacles and scoria ramparts. Scoria are dark grey in colour, porphyritic, with a well vesiculated core, locally welded and intercalated with coarse-ash beds. Lavas are black in colour, massive and autobrecciated at the base and top, with local columnar jointing.

### Stop 2.4: The Rio Corbore lava flow (40°43'31.40"N; 13°56'30.50"E)

Continuing the road towards the village of Fiaiano and turning northwards in the SS270, a spectacular 30 m high lava front outcrops at Rio Corbore locality (Fig. 29a). This lava flow has been emitted at about 5 ka by a vent located at Spalatriello locality and now buried by the Arso volcanic edifice. The highly viscous lava ended its run against a N-S trending pre-existent fault scarp cutting the Piano Liguori Tephra (Fig. 29b). The road cut exposes the massive structure of the lava and the internal columnar jointing.

The Piano Liguori Tephra is the product of a phreatomagmatic explosive eruption dated between 5.5 and 5 ka and consist of a succession of fine-grained and cross laminated pyroclastic-surge beds, with lenses of rounded-to-subangular pumice clasts. Deposits younger than 3 ka (Cannavale and Cretaio Tephra; de Vita et al., 2010) overlie a paleosol at the top of both Rio Corbore Lavas and Piano Liguori Tephra.

Turning towards south-west the road crosses both landslide deposits



Fig. 29 – Rio Corbore lava flow (~ 5 ka) at Spalatriello locality (a) and Piano Liguori Pyroclasts (b; 5.5 ka).



and volcanic centres of the last 10 ka of activity, such as the Molara scoria cone (dated 6<sup>th</sup>-5<sup>th</sup> century BC.; Buchner, 1986) and the Vateliero maar (5<sup>th</sup>-4<sup>th</sup> century BC; de Vita et al., 2010). Close to Piedimonte locality the road goes along the volcanic edifice of Costa Sparaina, a viscous lava dome dated 4 ka and displaced by a N-S trending fault (Vezzoli, 1988). After the Barano town the geological landforms change and the main outcropping lithologies are landslide deposits due to the gravitational instability of Mt. Epomeo southern slope.

### Stop 2.5: The Serrara belvedere (40°42'32.00"N; 13°53'33.20"E)

The view from 'belvedere' of Serrara sweeps from the Fontana basin to the east, to Punta Chiarito to the west, giving the opportunity to take a look to the morphological evolution of the southern slopes of Mt. Epomeo (Fig. 30).



The evolution of the so-called Serrara-Fontana basin, the concave, horse-shoe shaped southern flank of Mt. Epomeo (Fig. 31) is strictly linked to the caldera resurgence and to the progressive remobilization of the sedimentary and loose pyroclastic deposits mantling the Green Tuffs, occurred during the uplift of the resurgent blocks.

Tibaldi e Vezzoli (2004) describes a succession of debris avalanche deposits occurred within this basin. Thanks to the <sup>14</sup>C dating of two paleosols (8590 ± 110 a and 5690 ± 60 a) intercalated with debris avalanche deposits, the authors place the three most important episodes of avalanching between

Fig. 30 - View of Fontana area and Maronti beach from Serrara belvedere.

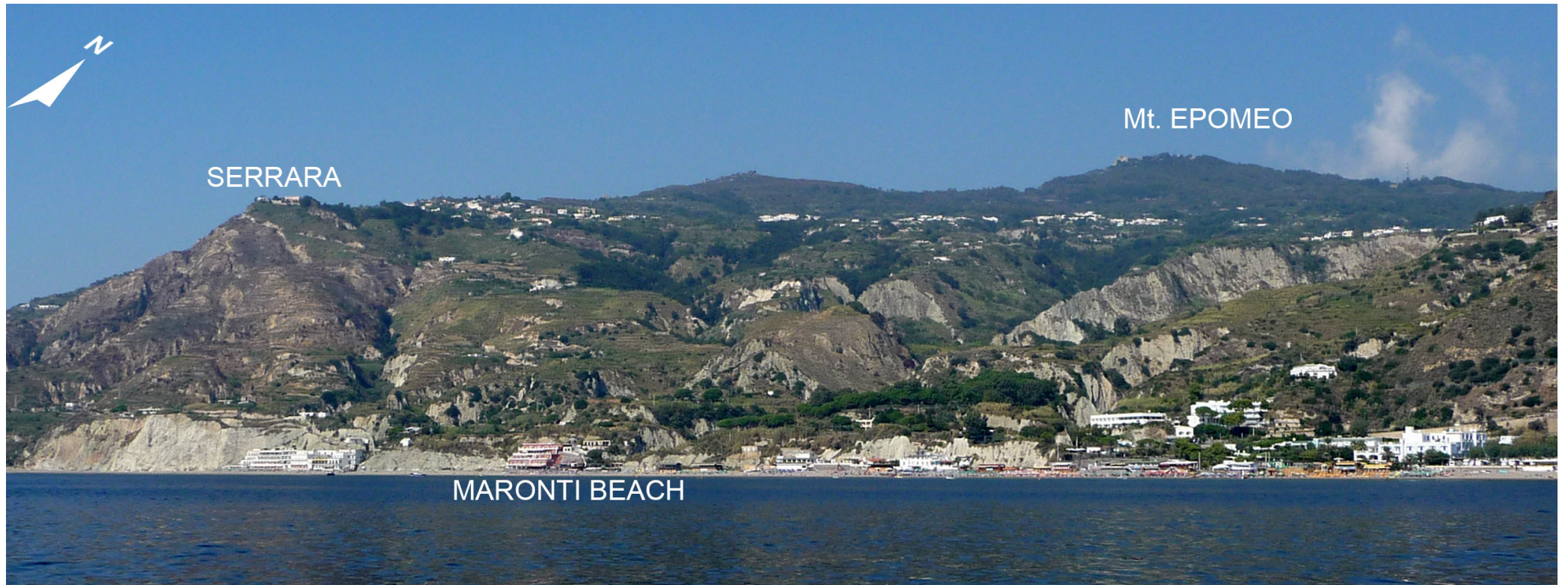


Fig. 31 - View from the sea of the Serrara-Fontana basin (southern slope of Mt Epomeo).

8.6 e 5.7 ka. They also identify seven older and minor landslide events, occurred between 33 e 8.6 ka, and seven minor events in the past 5.7 ka.

The angle of dip of the detachment surfaces of the debris avalanche deposits suggests that some of these could extend below the sea level, in agreement with the evidence of submarine landslide deposits recognized by other authors by means of bathymetric surveys and drillings (Chiocci and de Alteriis, 2006; de Alteriis and Violante, 2009).

Looking toward the south-west, outside the Serrara-Fontana basin, the area between Sant'Angelo and Punta Chiarito presents some interesting aspects, as already stated in stop 1.7.

This area is characterized by several landslides and mudflows deposits intercalated with pyroclastic deposits attributed to the Chiarito Tephra and to an explosive eruption (likely the Cretaio Tephra) dated about 2 ka.



The upper part of the landslide sequence that underlies the Chiarito Tephra contains artefacts of the VIII-VII century B.C. (Gialanella, 1998). This uppermost part of the sequence is a thick, diffusively humified, alluvial succession, with two interbedded undefined ash layers (de Vita et al., 2006). It contains several fragments of pottery and remains of meals (mollusk shells and ovine bones) mixed with charred wood, related to a Greek settlement of the VII century B.C. (Gialanella, 1998). Above this sequence, a debris- and rock-slide deposit with archaeological materials of the VII century B.C., lies directly below the Chiarito Tephra, from which it is separated by a thin and poorly developed paleosol (de Vita et al., 2006).

The Chiarito Tephra grades upwards into a humified surface that contains the remnants of a Greek settlement dated to the VII-VI century B.C. (Gialanella, 1998). This settlement was likely founded soon after the Chiarito Tephra eruption and was later buried by a debris-avalanche deposit, which is widely exposed in the study area (de Vita et al., 2006; Della Seta et al., 2012) and is often characterized by a basal erosional surface that truncates the upper part of the Chiarito Tephra.

The Chiarito Tephra itself (Fig. 32) is the product of a magmatic to phreatomagmatic eruption of trachytic magma occurred at Ischia in the 7<sup>th</sup> century BC (Gialanella, 1998). The vent for the Chiarito Tephra eruption is not visible in the field, but stratigraphic data indicates that it was located in the south-western area of Ischia island, likely on a NW-SE regional faults system bordering to south-west the Mt. Epomeo resurgent block. The vent position, together with the Zaro vents in the North-Western corner of the island, represents the unique evidence of volcanic activity during the last 10 ka outside the eastern sector of Ischia.

The Chiarito Tephra deposit shows strong analogies with the products of sub-plinian eruptions generated in the eastern sector of the Island during the past 5,000 years. In particular, the volume that is less than 0.1 km<sup>3</sup>, the type of deposits, consisting in pumice fallout and ash- to sand-sized flow beds, the dispersion axis along NE-SW direction and the vent location along a fault system bordering the Mt. Epomeo resurgent block, are common features with the Cretaio Tephra (Orsi et al., 1992). Furthermore, both eruptions erupted alkali-trachytic magmas, chemically and isotopically homogeneous, that experienced fluids contamination during water-magma interaction (Orsi et al., 1992) and likely derived from small-volume magma pockets evolving at shallow depth beneath Ischia (Piochi et al., 1999).

### Stop 2.6: The Zaro area (40°45''04.00'N; 13°52''38.50'E)

In the north-western edge of the island, the SS270 road crosses at Marecocco locality the volcanic vents which originated the main lava flows forming the Zaro promontory. This complex lava field, dated ~6 ka is composed



## CHIARITO TEPHRA

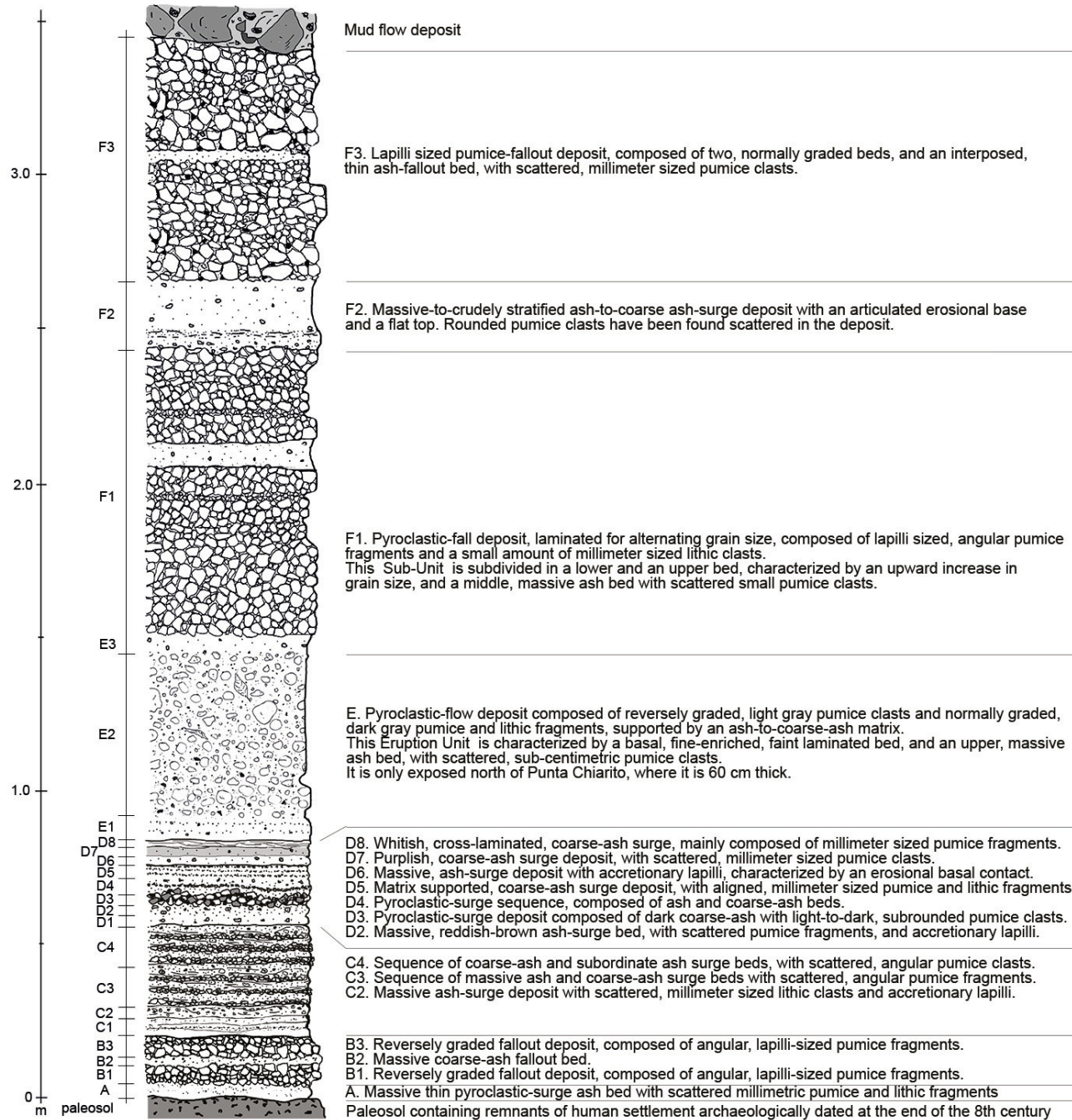


Fig. 32 - Description of Punta Chiarito Tephra pyroclastic deposit (7<sup>th</sup> century BC; modified after de Vita et al., 2010).

of several high aspect-ratio lava flows, lava domes and scoria cones from vents aligned along N-S, NE-SW and NW-SE trending faults at Marecocco, Caccaviello and Cavallaro locality (Figs 3, 22, and 33). In some cases, the extrusion occurred along the flanks of pre-existing hills, producing asymmetric domes and very viscous, low-mobility and high aspect-ratio lava flows. The basal lava flow is

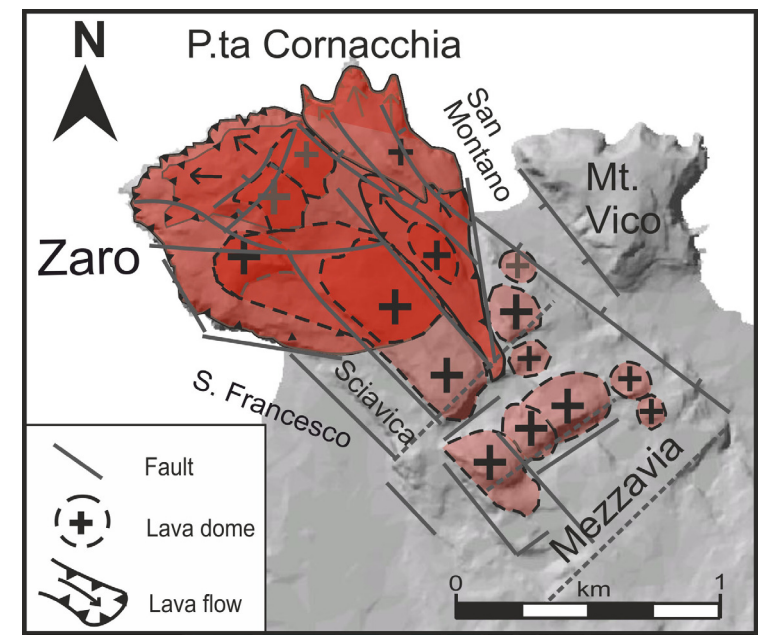


Fig. 33 - The Zaro area sketch map.



well visible at the beach of S. Francesco and at northern point of the promontory and it represents the most porphyritic lava body of all the lava field, with well-developed aggregates of feldspar crystals and subordinate pyroxenes inside a mainly microcrystalline ground-mass. All lavas are light grey in colour and due also to their very similar mineralogical and textural characteristics, have been interpreted as products of the same volcanic activity. Feeding dikes are intruded into a massive pyroclastic current deposit exposed along the southern side of the Zaro peninsula, at Sciavica locality.

### 3<sup>rd</sup> day - The Mt. Epomeo: caldera-forming eruptions, volcano-tectonic evolution and slope-instability

#### Stop 3.1: Purgatorio locality: the Mt. Nuovo DSGSD (40°44"50.15'N; 13°52"23.15'E)

The Mt. Nuovo DSGSD (Della Seta et al., 2012; 2015; Marmoni et al., 2017) covers an area of about 1.6 km<sup>2</sup> on the north-western flank of the Mt. Epomeo resurgent block and has been identified on the basis of diagnostic features (Fig. 34), such as: (a) significant counterslope terraces and scarps delimited by NE-SW, ENE-WSW and N-S-trending major fault segments; (b) bulging of the slope foot of the deformed block; and (c) occurrence of mass movements with a radial pattern along the slopes of the deformed block. The Mt. Nuovo block is a displaced portion of the rock sequence exposed along the western slope of Mt. Epomeo, which includes, from base upwards, the Mt. Epomeo Green Tuff (MEGT), the Mt. Epomeo Tuffite (produced by reworking of the MEGT in a submarine environment; Vezzoli, 1988) and a portion of the Colle Jetto Formation (a succession of marine siltstones and sandstones; Vezzoli, 1988). In addition, it is presently affected by a displacement rate in the order of magnitude of millimetres per year (Manzo et al., 2006).

The Mt. Nuovo DSGSD is detected as an ongoing gravity-induced deformational process that results from a MRC and results in a corollary of minor mass movements that were observed during the 4th century BC (Buchner 1986; Del Prete and Mele 2006).

Based on a geological, geomorphological, and geophysical reconstructions, Della Seta et al. (2015) estimated the volume of rock involved to be 190 Mm<sup>3</sup>. These authors also suggested that the DSGSD is accommodated by a low angle, 250 m deep shear zone, leading to a mainly translational mechanism. Such ongoing deformation is clearly seen in the bulging and opening of deep trenches (Fig. 34) that is superimposed on and filled by detrital materials, a direct consequence of the tensile stress field acting in this sector. In particular, the Mt. Nuovo DSGSD can be classified as a structurally-defined compound "constrained at toe" slide ("type E" Hungr



and Evans, 2004) in which the main rupture surfaces contain high-angle joint sets. Based on the reconstructed model, the basal shear zone does not appear to be controlled by any lithological or structural discontinuity, suggesting that different processes must explain its propagation. Considering the geo-structural similarities

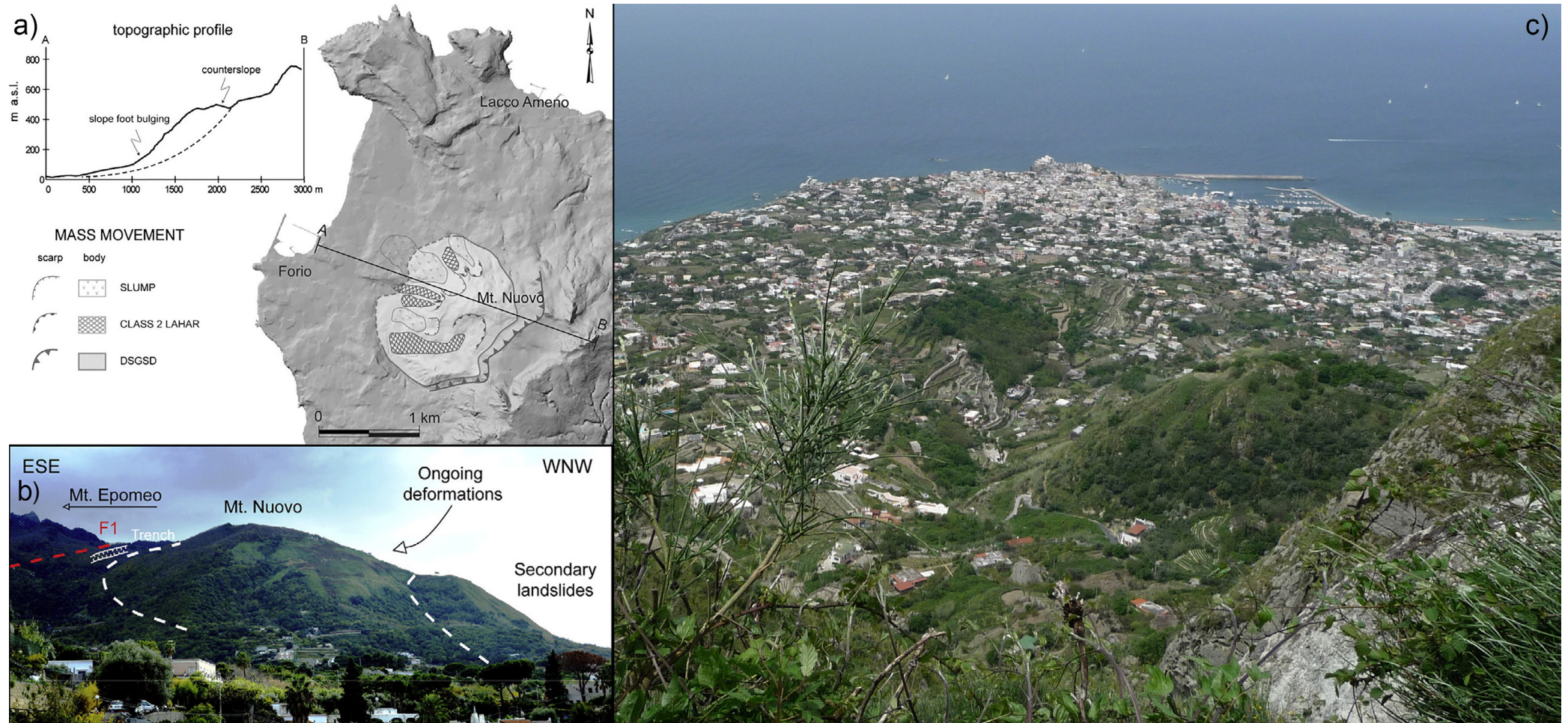


Fig. 34 – a) Plain view and topographic profile of diagnostic features of Mt. Nuovo DSGSD minor mass movements such as a significant counterslope scarp (delimited by NE-SW-, ENE-WSW- and N-S-trending major fault segments) and bulging of the slope foot of the deformed block, are evidenced in (after Della Seta et al., 2012). b) panoramic view from Forio of the Mt. Nuovo area involved in the ongoing gravitational deformation. Schematic traces of gravitational shear zone are shown as white dashed lines (after Marmoni et al., 2017). c) panoramic view from Mt. Epomeo of the Mt. Nuovo and Forio area.



(i.e. faults and joints) between the DSGSD at Mt. Nuovo and adjacent historic debris avalanches (Zaniboni et al., 2013) and the possible evolution of rock masses affected during their latest stages of MRC, it is likely that ongoing slope deformation involves the residual portion of a wider deforming block that had only partially achieved the conditions for collapse.

The Mt. Nuovo block is interested by pervasive high angle conjugated systems and low-angle sets of discontinuities. The main joint sets are a NS  $\pm 10^\circ$  trending system dipping westward around  $50^\circ$  and a NE-SW oriented set dipping  $20-30^\circ$  to SE. The high-angle planes are related to both major regional tectonic systems and local systems responsible for the resurgence of the Mt. Epomeo, while the low-angle ones correspond to gravitational shear planes.

The most pervasive systems also control the widespread landslide processes affecting the Mt. Nuovo slope as they are located at the edge of the main escarpments, where discontinuities isolate large unstable blocks, such as those identified in the Falanga plain. The joint trends have a direct correspondence in the morphological trenches observed upslope from the deformed volume, where they developed parallel to the slope suggesting a gravitational origin. The alignment of the aforementioned landforms with the main tectonic elements suggests a main tectonic control: pre-existing discontinuities, as well as the mechanical behaviour of MEGT and its failure modes (Marmoni et al., 2017), combined with high slope gradient, led to a slow mass rock creep process that evolved in a shear-zone driven deep landslide (Zaniboni et al., 2013). The pre-existing tectonic elements, genetically related to caldera resurgence, also provide preferential paths for geothermal fluids circulation, which in this part of the island is particularly active. Rising fluids either reach the surface at the top of the fault, or move laterally through discontinuities and high permeability layers, determining the hydrothermal alteration of the rock mass and the deterioration of its mechanical properties (Marmoni et al., 2017, Heap et al., 2018). This ultimately increases the proneness to the failure of the Mt. Nuovo block. Due to the lithological and structural characteristics of the Mt. Nuovo block, as well as their similarity with those characterizing already occurred debris avalanches on the island, it is possible to assume a generalized collapse of the slope as a possible ultimate scenario for the Mt. Nuovo landslide evolution.

According to Zaniboni et al. (2013), the possible evolution of the active Mt. Nuovo slope deformations toward a generalized collapse could produce tsunami wave able to reach high speeds (30 m/s) and height (more than 5 m) and therefore configuring significant risk conditions for the coasts of both the island and the Campania region.



## Stop 3.2: The Forio area: Debris avalanches and lahars of the western slopes of Mt. Epomeo (40°44"05.50'N; 13°51"58.80'E)

The Falanga debris/rock avalanche (IV century BC).

The recognised debris/rock avalanche deposits (Della Seta et al., 2012) consist of chaotic masses of matrix-supported megaclasts up to several metres in diameter (Fig. 27a). The largest megaclasts and blocks, responsible for the hummocky topography, are mainly composed of MEGT (Fig. 35a) and epiclastic deposits, the dominant lithology in the debris avalanche source areas. The blocks, although deformed, still preserve many of the primary textures. The clasts (<1 m) are tuff, epiclastic blocks, siltstone and lava fragments incorporated by the avalanche during its movement and are representative of the rocks exposed at a lower elevation compared with the source areas. Jigsaw cracks, although not very frequent, occur in both blocks and metric fragments. Due to the presence of large hummocks,

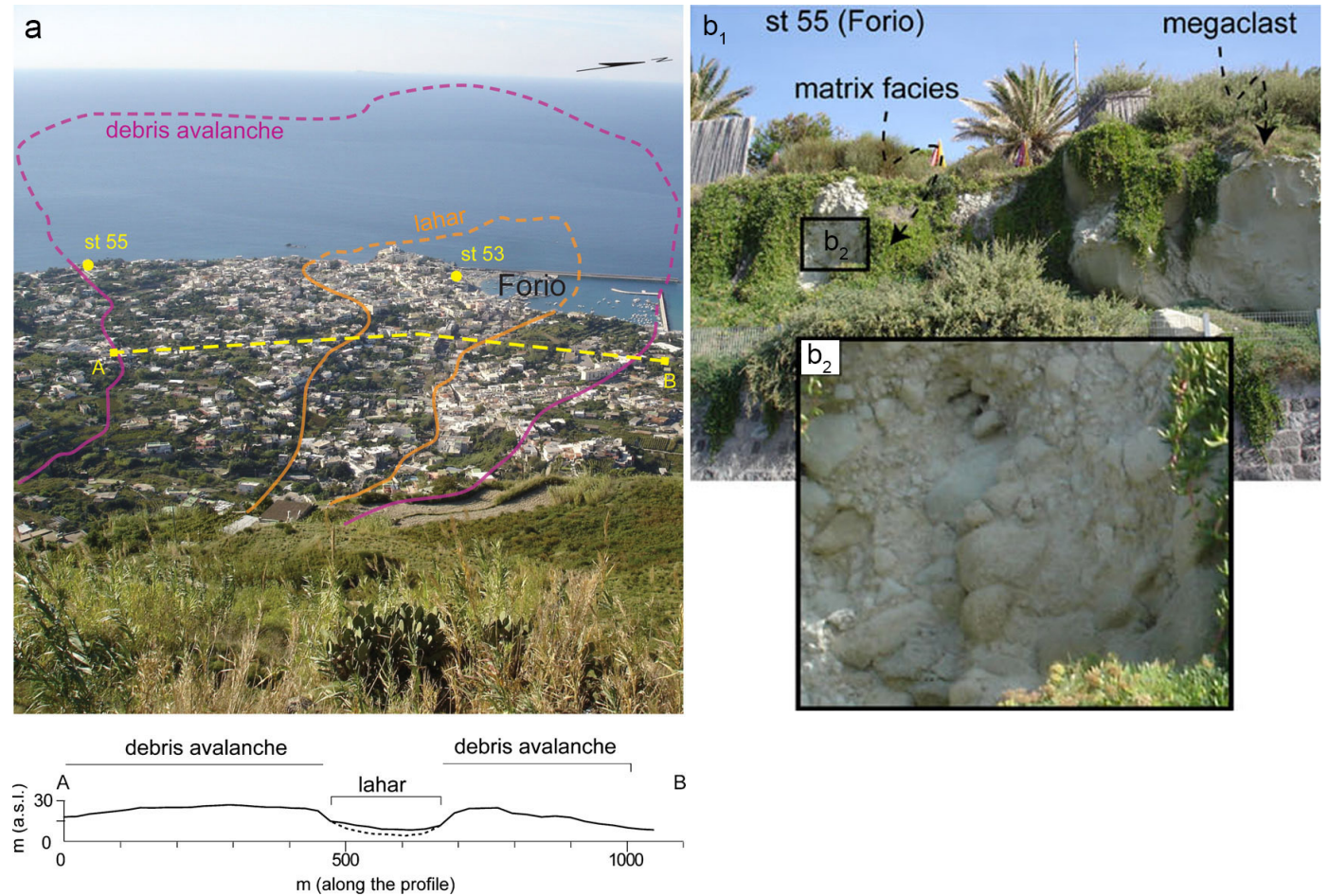


Fig 35 - a) The Falanga debris avalanche (IV century BC) and the superimposed deposit of the Forio Class 2 lahar (IV century BC). Due to the water content of the flow, the lahar body is more elongated in the plan view and has a flattish surface with respect to the debris avalanche body. As outlined by the topographic profile, the lahar body is channelled in a scar cutting the underlying debris avalanche body. b) Major features of the debris avalanche deposits: b<sub>1</sub>) Megaclast, up to several metres in diameter, resting in the matrix facies; b<sub>2</sub>) The matrix facies are generally poorly sorted, vesicular and massive. Modified after Della Seta et al. (2012).



debris/rock avalanche deposits are characterized by such highly irregular and rough surfaces that often they can be recognized even in densely urbanized areas. The matrix, generally poorly sorted, vesicular and massive (Fig. 35b), is composed of a chaotic and heterogeneous mixture of relatively fine particles, locally enriched in coarser clasts, usually concentrated in swarms. These swarms almost lack fine-grained material, which is present only as a coating around the larger sub-rounded clasts. Close to the base of the debris avalanche deposits, the matrix is laminated, well sorted and finer grained, does not contain large clasts and shows evidence of soft sediments deformation.

The areas covered by debris avalanche deposits range from 0.9 to 8.3 km<sup>2</sup>, with local subaerial thickness (estimated where the base is exposed) ranging between 10 and 25 m.

The slopes along the western side of Mt. Epomeo resurgent block, very prone to failure because of their lithological and structural characteristics, generated a large amount of debris flows and debris/rock avalanches, particularly during the 4<sup>th</sup> century BC, when also the Mt. Nuovo DSGSD was already documented (Buchner, 1986; Del Prete and Mele, 2006).

A step-like collapse started at the summit of the west-facing Mt. Epomeo steep slope, isolating the Falanga and Mt. Nuovo blocks. The collapsing of part of the Falanga block produced a large debris/rock avalanche that entered the sea (D'Argenio et al., 2004; Chiocci et al., 2006; de Alteriis and Violante, 2009), causing a forward coastline shift of some hundreds of meters (Rittmann and Gottini, 1980).

The Falanga debris/rock avalanche is a wide body with hummocky surface well visible also in the submerged part. It is a massive and ungraded, chaotic deposit, locally laminated at a large scale, due to internal shearing. Lenses and swarms of coarser material are present. The deposit is supported by a grey-greenish matrix and is very poorly sorted, with embedded a variable amount of sub-rounded, medium- to block- to boulder-sized clasts. Clasts are locally concentrated in swarms, where they are in contact to each other with a lesser amount of matrix. Hummocks are usually made of large MEGT and epiclastic boulders up to 4 m in diameter and are uniformly distributed over the surface of both emerged and submerged parts of the deposit.

The source detachment area of the Falanga debris/rock avalanche (IV century BC), as well as most of those occurring along the rim of the northern, north-western and south-western slopes of the Mt. Epomeo resurgent block, instead of having the typical horseshoe shape, is defined by intersecting rectilinear lineaments representing the emergence of portions of the NE/SW and NW/SE-trending high-angle fault planes generated during resurgence (Della Seta et al., 2012; Fig. 36).



### The Forio Class 1 lahar (IV century BC).

Deposits of class 1 lahars are generally fine- to medium-grained, matrix-supported, ungraded, massive, chaotic and poorly sorted bodies, containing variable amounts of cobbles and pebbles of MEGT, tuffite and lava. In places, they include blocks up to 5 m in diameter, which in some cases preserve the stratification of pyroclastic sequences, and rounded pumice clasts, either scattered or concentrated in swarms. The degree of alteration influences the colour of the matrix and is higher where fracturing of the source rocks is more pervasive and hydrothermal circulation is more widespread. The matrix of lahar deposits is usually vesicular, with local water escape structures; they are, less frequently partially lithified. Textural characteristics, size and hydrothermal alteration, despite the lack of grainsize data, suggest that the class 1 lahar deposits are similar to those of cohesive debris flows.

The areas covered by the mapped class 1 lahar deposits range from 0.2 to 1.1 km<sup>2</sup>, with a maximum thickness, only approximately estimated as the base of the deposits is never exposed, between 5 and 20 m (Della Seta et al., 2012).

As many of the other lahars of both Class 1 and 2, the Forio lahar was activated along the western flank of the Mt. Epomeo resurgent block. These lahars mostly detached in areas of intense soil degassing, involved the slope talus and flowed on the top of debris/rock avalanche deposits as water-saturated flows. Since lahars often flowed on top of debris/rock avalanche

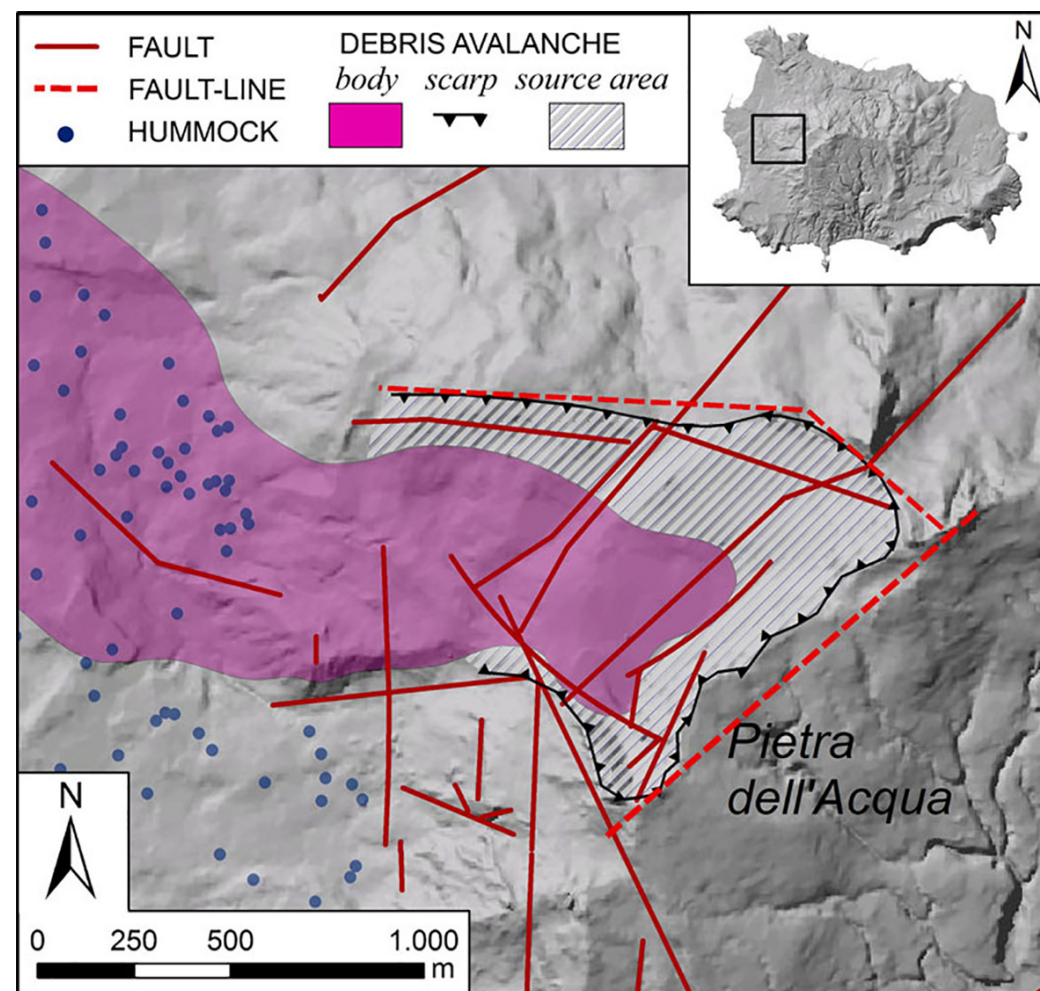


Fig. 36- Debris avalanche source areas are often not characterized by the typical horseshoe shape, but they are defined by the intersection of at least two (or more) fracture systems, likely active during resurgence. Dashed lines evidence trend and position of the original fault scarps reworked by detachment. After Della Seta et al. (2012).



deposits not significantly eroded by surface running waters, it is likely that the scars in which they lie were eroded by the moving water-saturated current. Nonetheless, there are no evidence, besides the information coming from historical chronicles, to infer whether or not debris/rock avalanches and superimposed lahars are genetically associated within the same events. Textural characteristics of the deposits, along with the strong hydrothermal alteration of the rocks in their source areas, suggest that these currents likely were cohesive debris flows. Also, the texture of the deposits can give information on the relative water content of the currents and consequently on their erosive power (Vallance, 2015). Differences in water content may be highlighted as well by the different surface morphology of the lahar deposits. For example, since the Forio lahar deposit is characterised by a flattish surface and is channelled in a deeper scar, the current from which it was laid down (Fig. 35b) is inferred to have been water-rich, as it is also supported by the textural characteristics of the deposits.

The Forio lahar is an elongated body composed of a massive and chaotic deposit, with water-escape structures. It is coherent or locally partially lithified, greenish-grey, matrix-supported, almost monolithologic with sub-rounded epiclastic blocks up to 1.5 m in diameter in a tuffite matrix (Della Seta et al., 2012).

As a conclusion it is worth noting that in case of reactivation uplift event in response to renewal of magmatic activity, the Mt. Nuovo DSGSD block and some densely fractured areas characterised in turn by steep slopes, high geothermal gradients and deep hydrothermal alteration along the western and northern flanks of Mt. Epomeo could be possible source areas for new catastrophic debris/rock avalanches.

Slope instability, and in particular debris avalanches and lahars with their high destructive power, have to be considered in any attempt to contribute to long-term assessment of volcanic and related hazards at Ischia. In addition to the catastrophic effects that such phenomena could have inland, they have the potential to generate large tsunamis that could affect also the neighbouring and densely inhabited coastal portion of the Neapolitan area (Della Seta et al., 2012).

### Stop 3.3: Pietra Martone and Bosco della Falanga (40°43"09.00'N; 13°53"03.00'E)

Close to Fontana town, at Pantano locality, the road to Pietra Martone and then to the Falanga locality gives the opportunity to see outcrops of ignimbrite deposits of the Mt. Epomeo Green Tuff eruptions. The path crosses trough Green Tuff blocks, modelled by wind erosion and characterized by sub-vertical rock faces due to the resurgence faults. Downslope Serra locality, a fumarole field takes place (Donna Rachele fumaroles). It is one of the widest and high-temperatures fumarole site of Ischia island.



Fig 37 - The Falanga wood at the back the 200 m high Green Tuff vertical fault face.

Passed the Serra locality the path goes downhill bringing to the Falanga wood, which represents a step-fault delimited by an impressive 200 m high Green Tuff vertical face (Fig. 2; Fig. 37). The top of this fault-face is the highest point of the island named Capo dell'Uomo (787 m a.s.l.). Downslope the flat step-fault of Falanga there is the DSGSD Monte Nuovo block, discussed at stop 3.1. Along the exposed fault-planes the intracaldera ignimbrite facies of the Mt. Epomeo Green Tuff (MEGT) are visible (Brown et al., 2008). They are composed of two indurated trachytic ignimbrite flow-units (Lower and Upper MEGT; Fig. 38) exposed in steep fault scarps around the Monte Epomeo resurgent block.

Vezzoli (1988) obtained a K/Ar age of  $\sim 55$  ka for the UMEGT intracaldera ignimbrites. The Lower MEGT is  $>70$  m thick and is exposed only on the western flank of the most uplifted part of the resurgent block (Rione Bocca). Step-faulting associated with resurgence (Orsi et al. 1991) suggests that it lies below the present level of exposure in the north-western parts of the block. The Lower MEGT overlies marine volcanoclastic sandstones and conglomerates, and it comprises a basal heterometric lithic breccia up to 20 m thick that passes up into a  $\sim 50$  m thick massive ignimbrite. The lithic population in the breccia comprises lapilli, blocks and boulders of phonolite and trachyte lava, tuff, lapilli-tuff, coarse grained holocrystalline feldspar-phyric sub-volcanic rocks, hydrothermally altered clasts and scattered sandstone clasts. Juvenile material in the Lower MEGT comprises brown-black irregular to fluidal-shaped dense and poorly vesicular spatter, abundant porphyritic tube pumice,

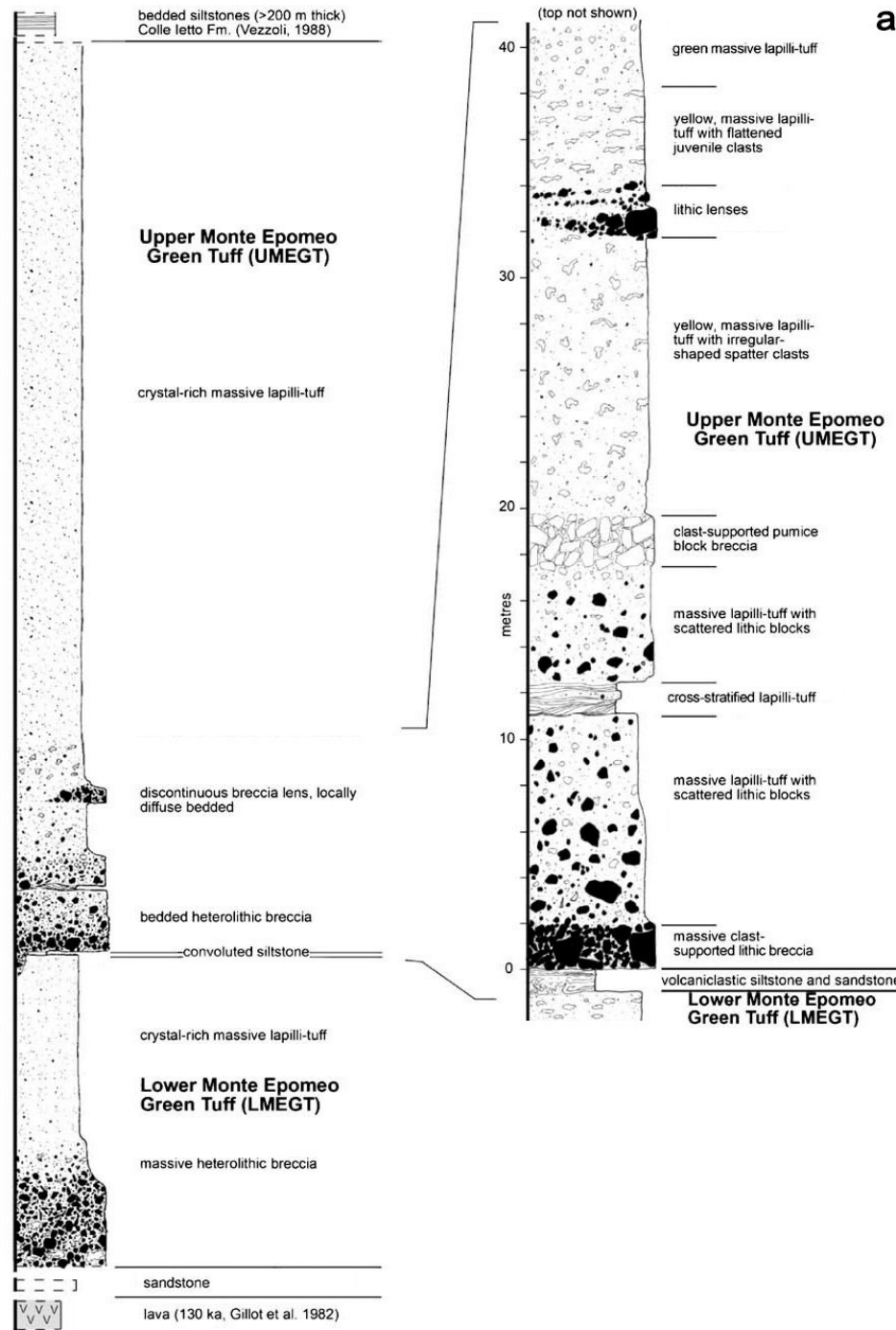


Fig. 38 - Composite vertical sequence of the Monte Epomeo Green Tuff (a; modified after Brown et al., 2008) and pictures of its outcrops at Rione Bocca up to Monte Epomeo (b and c).

<https://doi.org/10.3301/GFT.2018.03>



and large feldspar (<15 mm) and biotite (<6 mm) free crystals. The altered ash matrix is strongly enriched in crystals relative to the juvenile material.

The Upper MEGT (Fig. 38) is >200 m thick and is extensively exposed in the fault scarps around Monte Epomeo. Lower parts of the Upper MEGT at Rione Bocca comprise, from base to top, clast-supported lithic breccia, boulder-bearing ignimbrite, cross-stratified and dune-bedded ignimbrite and spatter-bearing ignimbrite. The upper ~150 m consists of homogenous normally-graded massive ignimbrite with abundant pumice lapilli and blocks and minor lithic lapilli. Lithic and pumice lapilli become finer grained and less abundant upwards. Juvenile material is similar to that of the Lower MEGT. The Upper MEGT is unconformably overlain by laminated, bedded and locally fossiliferous marine volcanoclastic siltstones and sandstones (Colle Ietto Formation, Vezzoli 1988) which record the reworking of the MEGT tephra during post- or syn-eruptive flooding of the caldera (Vezzoli 1988; Barra et al. 1992). The contact between the Lower and Upper MEGT is discontinuously exposed at Rione Bocca. It is marked by a ~1 m thick unit of faintly laminated to massive, moderately to poorly-sorted vitric siltstones and fine- to coarse-grained sandstones. These sediments locally exhibit convoluted bedding. Elsewhere, the contact is marked by several metres of chaotically bedded whitish vitric siltstone and sandstone with broad local erosion surfaces and in which it is difficult to distinguish either the top of the Lower MEGT or the base of the Upper MEGT. To the north, the contact is marked by an erosion surface that cuts down >20 m into the Lower MEGT. Coarse lithic breccia lenses and scattered boulders occur in the Upper MEGT along this scour surface, but where they are absent the two-ignimbrite flow-units are indistinguishable. The contact is less obvious on the north-facing scarps of Monte Epomeo, but it may be marked by a discontinuous clast supported lithic breccia that overlies a massive yellow lapilli-poor ignimbrite that probably belongs to the Lower MEGT (Brown et al., 2008).

## References

- Acocella V. and Funiciello R. (1999) - The interaction between regional and local tectonics during resurgent doming: the case of the island of Ischia, Italy. *J. Volcanol. Geotherm. Res.*, 88, 109-123.
- Angiulli G., De Francesco A.M., Lomonaco L. (1985) - Nuovi dati geochimica sull'Isola di Ischia. *Mineral. Petrogr. Acta*, 29, 41-60.
- Bartole R., Savelli D., Tramontana M., Wezel F.C. (1984) - Structural and sedimentary features in the Tyrrhenian margin off Campania, Southern Italy. *Marine Geology*, 55 (3-4), 163-180, ISSN 0025-3227.
- Brown R.J., Orsi G., de Vita S. (2008) - New insights into Late Pleistocene explosive volcanic activity and caldera formation on Ischia (southern Italy). *Bull. Volc.*, 70(5), 583-603. <https://doi.org/10.1007/s00445-007-0155-0>.
- Brown R.J., Civetta L., Arienzo I., D'Antonio M., Moretti R., Orsi G., Tomlinson E.L., Albert P.G., Menzies M. (2014) - Assembly, evolution and disruption of a magmatic plumbing system before and after a cataclysmic caldera-collapse eruption at Ischia volcano (Italy). *Contrib. Mineral. Petrol.*, 168 (2), 1-23.
- Bruno P.P.G., de Alteriis G., Florio G. (2002) - The western undersea section of the Ischia volcanic complex (Italy, Tyrrhenian Sea) inferred by marine geophysical data. *Geophysical Research Letters*, 29 (9), <https://doi.org/10.1029/2001GL019304>.
- Buchner G. (1986) - Eruzioni vulcaniche e fenomeni vulcanotettonici di età preistorica e storica nell'isola d'Ischia. In: Centre Jean Bérard, Institut Français de Naples (ed), *Tremblements de terre, éruptions volcaniques et vie des hommes dans la Campanie antique*, 7, 145-188.
- Buchner G., Italiano A., Vita-Finzi C. (1996) - Recent uplift of Ischia, southern Italy. *Geol. Soc. Lond., Special Publications*, 110, 249-252
- Carlino S. (2012) - The process of resurgence for Ischia Island (southern Italy) since 55 ka: the laccolith model and implications for eruption forecasting. *Bulletin of Volcanology*, 74(5), 947-961.
- Carlino S., Cubellis E., Luongo G., Obrizzo F. (2006) - On the mechanics of caldera resurgence of Ischia Island (southern Italy). *Geol. Soc. Lond., Special Publications*, 269(1), 181-193.
- Casalini M., Avanzinelli R., Heumann A., de Vita S., Sansivero F., Conticelli S., Tommasini S. (2017) - Geochemical and radiogenic isotope probes of Ischia volcano, Southern Italy: Constraints on magma chamber dynamics and residence time. *American Mineralogist*, 102(2), 262-274. <https://doi.org/10.2138/am-2017-5724>.
- Catenacci V. (1992). Il dissesto geologico e geoambientale in No. 2089. Italia dal dopoguerra al 1990. *Memorie Descrittive della Carta Geologica d'Italia*, Servizio Geologico Nazionale, 47, 301 pp.
- Chigira M. (1992) - Long-term gravitational deformation of rocks by mass rock creep. *Eng. Geol.*, 32, 157-184.
- Chiocci F. L. and de Alteriis G. (2006) - The Ischia debris avalanche: first clear submarine evidence in the Mediterranean of a volcanic island prehistorical collapse. *Terra Nova*, 18(3), 202-209.
- Civetta L., Gallo G., Orsi G. (1991) - Sr- and Nd- isotope and trace-element constraints on the chemical evolution of the magmatic system of Ischia (Italy) in the last 55 ka. *J. Volcanol., Geotherm. Res.*, 46, 213-230.
- Crisci G.M., De Francesco A.M., Mazzuoli R., Poli G., Stanzione D. (1989) - Geochemistry of recent volcanics of Ischia Island, Italy: Evidences of fractional crystallization and magma mixing. *Chem. Geol.*, 78, 15-33.

- Cubellis E., Luongo G. (1998) - Sismicità storica dell'isola d'Ischia. In: Istituto poligrafico e zecca dello Stato (Ed.), Il terremoto del 28 luglio 1883 a Casamicciola nell'isola d'Ischia, 49-57.
- D'Antonio M., Tonarini S., Arienzo I., Civetta L., Dallai L., Moretti R., Orsi G., Andria M., Trecalli A. (2013) - Mantle and crustal processes in the magmatism of the Campania region: inferences from mineralogy, geochemistry, and Sr-Nd-O isotopes of young hybrid volcanics of the Ischia island (South Italy). *Contrib. Mineral. Petrol.*, 165, 1173. <https://doi.org/10.1007/s00410-013-0853-x>.
- D'Argenio B., Pescatore T., Scandone P. (1973) - Schema geologico dell'Appennino meridionale (Campania e Lucania). *Acc. Naz. Linc.*, 182, 49-72.
- D'Argenio B., Aiello G., de Alteriis G., Milia A., Sacchi M., Tonielli R., Budillon F., Chiocci F., Conforti A., De Lauro M., d'Isanto C., Esposito E., Ferraro L., Insinga D., Iorio M., Marsella E., Molisso F., Morra V., Passaro S., Pelosi N., Porfido S., Raspini A., Ruggieri S., Terranova C., Vilardo G. and Violante C. (2004). Digital elevation model of the Naples bay and adjacent areas, eastern Tyrrhenian sea. *Atlas Italian Geologic Mapping*, 32IGC, Firenze, August 2004.
- de Alteriis G. and Violante C. (2009) - Catastrophic landslides off Ischia volcanic island (Italy) during prehistory. *Geol. Soc. Lond., Special Publications*, 322, 73-104.
- De Novellis V., Carlino S., Castaldo R., Tramelli A., De Luca C., N. Pino A., Pepe S., Convertito V., Zinno I., De Martino P., Bonano M., Giudicepietro F., Casu F., Macedonio G., Manunta M., Cardaci C., Manzo M., Di Bucci D., Solaro G., Zeni G., Lanari R., Bianco F., Tizzani P. (2018) - The 21 August 2017 Ischia (Italy) earthquake source model inferred from seismological, GPS, and DInSAR measurements. *Geophysical Research Letters*, 45, 2193-2202. <https://doi.org/10.1002/2017GL076336>.
- de Vita S., Sansivero F., Orsi G., Marotta E. (2006) - Cyclical slope instability and volcanism related to volcano-tectonism in resurgent calderas: the Ischia island (Italy) case study. *Eng. Geol.*, 86, 148-165.
- de Vita S., Sansivero F., Orsi G., Marotta E., Piochi M. (2010) - Volcanological and structural evolution of the Ischia resurgent caldera (Italy) over the past 10 ka. In: Groppelli G. and Viereck L. (Eds.) "Stratigraphy and geology in volcanic areas", GSA Book series, Special paper, 464, 193-239.
- de Vita S., Di Vito M.A., Gialanella C., Sansivero F. (2013) - The impact of the Ischia Porto Tephra eruption (Italy) on the Greek colony of Pthekoussai. *Quat. Int.*, 303, 142-152. <http://dx.doi.org/10.1016/j.quaint.2013.01.002>.
- Del Gaudio C., Aquino I., Ricciardi, Ricco C., Scandone R. (2010) - Unrest episodes at Campi Flegrei: A reconstruction of vertical ground movements during 1905-2009, *J. Volcanol. Geotherm. Res.*, 195, 48-56, <https://doi.org/10.1016/j.jvolgeores.2010.05.014>.
- Del Prete S., Mele R. (1999) - L'influenza dei fenomeni d'instabilità di versante nel quadro morfoevolutivo della costa dell'isola d'Ischia. *Boll. Soc. Geol. It.*, 118, 339-360.
- Del Prete S., Mele R. (2006) - Il contributo delle informazioni storiche per la valutazione della propensione al dissesto nell'Isola d'Ischia. *Rend. Soc. Geol. It., Nuova Serie*, 2, 29-47.
- Della Seta M., Marotta E., Orsi G., de Vita S., Sansivero F., Fredi P. (2011) - Slope instability induced by volcano-tectonics as an additional source of hazard in active volcanic areas: the case of Ischia island (Italy). *Bull. Volcanol.*, 74(1), 79-106, <https://doi.org/10.1007/s00445-011-0501-0>.

- Di Martire D., de Rosa M., Pesce V., Santangelo M.A., Calcaterra D. (2012). Landslide hazard and land management in high-density urban areas of Campania region, Italy. *Nat. Hazards Earth Syst. Sci.*, 12 (4), 905-926. <http://dx.doi.org/10.5194/nhess-12-905-2012>.
- Di Napoli R., Martorana R., Orsi G., Aiuppa A., Camarda M., De Gregorio S., Gagliano Candela E., Luzio D., Messina N., Pecoraino G., Bitetto M., de Vita S., Valenza M. (2011) - The structure of a hydrothermal system from an integrated geochemical, geophysical and geological approach: the Ischia Island case study. *Geochem. Geophys. Geosyst.*, 12(7), <https://doi.org/10.1029/2010GC003476>.
- Finetti I. and Morelli C. (1974) - Esplorazione sismica a riflessione dei Golfi di Napoli e Pozzuoli. *Boll. Geof. Teor. Appl.*, 16, 175-222.
- Gialanella C. (1998) - Pithecusa: una fattoria greca arcaica a Punta Chiarito. *Ass. Internazionale Amici di Pompei, Archeologia e Vulcanologia in Campania*, pp. 87-96.
- Heap M., Kushnir A., Griffiths L., Wadsworth F., Marmoni G. M., Fiorucci M., Martino S., Baud P., Gilg H. A., Reuschlé T. (2018) - Fire resistance of the Mt. Epomeo Green Tuff, a widely-used building stone on Ischia Island (Italy). *Volcanica*, 1(1), 33-48. <https://doi.org/10.30909/vol.01.01.3348>.
- Hungr O. and Evans S.G. (2004) - Entrainment of debris in rock avalanches: An analysis of a long run-out mechanism. *GSA Bulletin*, 116(9-10), 1240-1252. <https://doi.org/10.1130/B25362.1>.
- Ippolito F., Ortolani F., Russo M. (1973) - Struttura marginale tirrenica dell'Appennino campano: reinterpretazione di dati di antiche ricerche di idrocarburi. *Mem. Soc. Geol. Ital.*, 12, 227-250.
- Luongo G., Cubellis E., Di Vito M.A., Cascone E. (1995) - L'isola d'Ischia: dinamica e struttura del M. Epomeo. In Bonardi, G., De Vivo, B., Gasparini, P., Vallario, A., Cinquant'anni di attività didattica e scientifica del Prof. Felice Ippolito. Liguori Editore, Napoli.
- Marmoni G.M., Martino S., Heap M.J., Reuschlé T. (2017) - Gravitational slope-deformation of a resurgent caldera: New insights from the mechanical behaviour of Mt. Nuovo tuffs (Ischia Island, Italy). *Journal of Volcanology and Geothermal Research*, 345, 1-20. <https://doi.org/10.1016/j.jvolgeores.2017.07.019>.
- Manzo M., Ricciardi G.P., Casu F., Ventura G., Zeni G., Borgström S., Berardino P., Del Gaudio C., Lanari R. (2006) - Surface deformation analysis in the Ischia Island (Italy) based on spaceborne radar interferometry. *J. Volcanol. Geotherm. Res.*, 151(4), 399-416.
- Moretti R., Arienzo I., Orsi G., Civetta L., D'Antonio M. (2013) - The Deep Plumbing System of Ischia: a Physico-chemical Window on the Fluid-saturated and CO<sub>2</sub>-sustained Neapolitan Volcanism (Southern Italy), *Journal of Petrology*, 54(5), 951-984. <https://doi.org/10.1093/petrology/egt002>.
- Nappi R., Alessio G., Gaudiosi G., Nave R., Marotta E., Siniscalchi V., Civico R., Pizzimenti L., Peluso R., Belviso P., Porfido S. (2018) - The 21 August 2017 Md 4.0 Casamicciola Earthquake: First Evidence of Coseismic Normal Surface Faulting at the Ischia Volcanic Island. *Seismological Research Letters*; 89(4), 1323-1334. <https://doi.org/10.1785/0220180063>.
- Orsi G., Chiesa S. (1988) - The uplift of the Mt. Epomeo block at the island of Ischia (Gulf of Naples): geological and geochemical constraints. *Eos*, 69(44), 1473.

- Orsi G., Gallo G., Zanchi A. (1991) - Simple-shearing block resurgence in caldera depression. A model from Pantelleria and Ischia. *J. Volcanol. Geotherm. Res.*, 47, 1-11.
- Orsi G., Gallo G., Heiken G., Wohletz K., Yu E., Bonani G. (1992) - A comprehensive study of the pumice formation and dispersal: the Cretatio Tephra of Ischia (Italy). *J. Volcanol. Geotherm. Res.*, 53, 329-354.
- Orsi G., Piochi M., Campajola L., D'Onofrio A., Gialanella L., Terrasi F. (1996) - 14C geochronological constraints for the volcanic history of the island of Ischia (Italy) over the last 5,000 years. *J. Volcanol. Geotherm. Res.*, 71, 249-257.
- Orsi G., Patella D., Piochi M., Tramacere A. (1999) - Magnetic modelling of the Phlegrean volcanic district with extension to the Ponza Archipelago, Italy. *J. Volcanol. Geotherm. Res.*, 91, 345-360.
- Piochi M., Bruno G., De Astis G. (2005) - Relative roles of rifting tectonics and magma ascent processes: Inferences from geophysical, structural, volcanological, and geochemical data for the Neapolitan volcanic region (southern Italy), *Geochem. Geophys. Geosyst.*, 6, Q07005, <https://doi.org/10.1029/2004GC000885>.
- Piochi M., Civetta L., Orsi G. (1999) - Mingling in the magmatic system of Ischia (Italy) in the past 5ka. *Mineral. Petrol.*, 66, 227-258.
- Poli S., Chiesa S., Gillot P.Y., Gregnanin A., Guichard F. (1987) - Chemistry versus time in the volcanic complex of Ischia (Gulf of Naples, Italy): evidence of successive magmatic cycles. *Contrib. Mineral. Petrol.*, 95, 322-335.
- Poli S., Chiesa S., Gillot P.Y., Guichard F., Vezzoli L. (1989) - Time dimension in the geochemical approach and hazard estimation of a volcanic area: the Isle of Ischia case (Italy). *J. Volcanol. Geotherm. Res.*, 36, 327-335.
- Rittmann A. (1930) - Geologie der Insel Ischia. *Z. f. Vulkanol. Ergänzungsband*, 6.
- Rittmann A., Gottini V. (1980) - L'Isola d'Ischia - Geologia. *Boll. Serv. Geol. It.*, 101, 131-274.
- Sbrana A., Toccaceli R.M. (2011) - Carta Geologica dell'isola d'Ischia e Note illustrative. Regione Campania, Assessorato Difesa del Suolo. Litografica Artistica Cartografica. Firenze, 216 pp.
- Sepe V., Atzori S., Ventura, G. (2007) - Subsidence due to crack closure and depressurization of hydrothermal systems: a case study from Mt Epomeo (Ischia Island, Italy). *Terra Nova*, 19, 127-132. <https://doi.org/10.1111/j.1365-3121.2006.00727.x>.
- Santo A., Di Crescenzo G., Del Prete S., Di Iorio L. (2012) - The Ischia island flash flood of November 2009 (Italy): phenomenon analysis and flood hazard. *Phys. Chem. Earth*, 49, 3-17.
- Tibaldi A., Vezzoli L. (1997) - Intermittenza e struttura della caldera risorgente attiva dell'isola d'Ischia. *Il Quaternario*, *J. Quatern. Sci.*, 10(2), 465-470.
- Tibaldi A., Vezzoli L. (1998) - The space problem of a caldera resurgence: an example from Ischia Island, Italy. *Geologische Rundschau*, 87, 53-66.
- Tibaldi A., Vezzoli L. (2004) - A new type of volcano flank failure: The resurgent caldera sector collapse, Ischia, Italy. *Geophysical Research Letters*, 31, <https://doi.org/10.1029/2004GL020419>.
- Vallance J.W., Iverson R.M. (2015) - Lahars and Their Deposits. *The Encyclopedia of Volcanoes (Second Edition)*. Academic Press, 649-664, ISBN 9780123859389. <https://doi.org/10.1016/B978-0-12-385938-9.00037-7>.
- Vezzoli L. (1988) - Island of Ischia. *CNR Quaderni de "La ricerca scientifica"*, 114(10), 122 pp.

- Vezzoli L., Principe C., Malfatti J., Arrighi S., Tanguy J.C., Le Goff M. (2009) - Modes and times of caldera resurgence: The <10 ka evolution of Ischia Caldera, Italy, from high-precision archaeomagnetic dating, *J. Volcanol. Geotherm. Res.*, 186, 305-319.
- Zaniboni F., Pagnoni G., Tinti S., Della Seta M., Fredi P., Marotta E., Orsi G. (2013) - The potential failure of Monte Nuovo at Ischia Island (Southern Italy): numerical assessment of a likely induced tsunami and its effects on a densely inhabited area. *Bull. Volcanol.*, 75, 763. <https://doi.org/10.1007/s00445-013-0763-9>.